

XMM Optical Monitor

**MULLARD SPACE SCIENCE LABORATORY
UNIVERSITY COLLEGE LONDON**

Author: H. Kawakami

Mid term Report-B on the life time estimation of FM-intensifiers

<< Intense illumination of DEP_#8 intensifier >>

Document Number: XMM-OM/MSSL/TC/0057 30-Novemebr-99

Distribution:

XMM-OM Project Office

A Dibbens

Orig.

Mullard Space Science Laboratory

K Mason
A Smith
H Huckle
H Kawakami

ESTEC

R Much

DEP

SWIFT

T Kennedy
B Hancock
M Cropper

Mid term Report-B on the life time estimation of FM-intensifiers

<< Intense illumination of DEP_#8 intensifiers >>

10. Light source

A new light source was made for brighter and more accurate illumination. The problems associated with the former light source are;

- (a) The light source was a surface fluorescence panel driven by an AC 100V. It showed flickering synchronized with the 50Hz electric power.
- (b) The fluorescence from the light source was a problem to measure dark current of an image intensifier.
- (c) It was necessary to reduce brightness of the light source to calibrate absolute brightness of pinholes. The uniformity of the illumination was, however, not guaranteed when a very low voltage was applied. This inhibited accurate calibration.
- (d) The previous mask pattern employed 4 plastic ND1.2 filters to create brightness ratio of $1E+4.8$ among the pinholes. It, however, could create only $1E+3$, which was due to red leak of the cheap plastic ND filters.

The new light source employs 64 green LEDs to avoid fluorescence and flickering. The 64 LEDs were divided into 2 groups of 32 LEDs, and each of the 32 LEDs were connected together in series to be driven by one of the two identical current sources (see Fig 17). This approach allowed to handle only 100V DC in stead of 200V DC to light the 64 LEDs. The brightness can be changed to 10 fixed levels (+ dark). The 32 LEDs were covered with 4 sheets of diffuser to improve uniformity of the illumination (see Fig 18). A mask pattern with 11x11 pinhole array was located 46 mm above the diffuser. A green interference filter, whose pass band is 5300-5700Å, was placed beneath the mask pattern to cut red leak through ND filters. Four ND filters were stuck beneath each of the columns in the pinhole mask pattern to create 11 different brightness levels. The two of the four were glass ND1.0 filters, whose extreme low red leak was measured and confirmed by the manufacture. Other two were the previously used plastic ND1.2 filters. The latter two definitely have red leak, but should not be a problem in the attenuation level of $1E+2.4$ with the help of the green narrow band filter. The scattered light from the brightest pinholes overpowers the light from the faintest pinholes, because of the large difference of brightness (ratio= $1.8E4$). The brightest pinholes can be covered with an optional blackout material to obtain more accurate data for the faintest pinholes.

The 11x11 pinhole array was projected on right edge of the intensifier using a F/2 IPCS lens with the image reduction of 1.7. Diameter of the pinholes is 100µm on the mask.

This relatively large diameter was for providing sufficiently high intensity from the individual pinholes. Since the image was suffered from optical aberration due to strong curvature of the detector window, the pinhole diameter of the projected image varied from 60 to 70 μ m depending on the positions at the detector (best focused for the brightest pinholes). As the width of electron cloud inside the intensifier is 70-80 μ m, the change of diameter hopefully does not affect results much.

The pinhole array images were acquired with the MIC photon counting detector to determine the absolute brightness of individual pinholes at the 10 LED brightness levels. CCD camera format of 256(H)x100(V) was employed to enhance dynamic range of the MIC photon counting detector. It achieved the frame rate of 217.3251619Hz, in other word, the frame period of 4.6014ms. Since photons from a pinhole was missed during the frame transfer period, 0.2304ms, the duty ratio of was 94.993% ($= 1 - 0.2304\text{ms} / 4.6014\text{ms}$). Even with this fast frame rate, coincidence loss exceeds 10% if a pinhole emits in the rate of 50 events/sec. The dead time and the coincidence were corrected by the following equation,

$$x_{\text{real}} = FR * \{ -\ln(1 - x_{\text{det}}/FR) \} / (1 - FT/P)$$

where, x_{det} denotes detected events in a pinhole, x_{real} true number of events, FR the frame rate of the CCD camera, FT the duration of frame transfer, and P frame period of the CCD camera (ref. XMM-OM/ MSSSL/TC/0050 Nov '98).

The maximum brightness ratio among the pinhole columns and that among the different LED currents are more than $1\text{E}+4$. These are far beyond the coverage of the MIC detector. Therefore, brightness ratios between non-saturated pinholes only were determined at a LED brightness level. The ratios between other pinholes were measured by changing the LED brightness. The optional blackout material was used in these measurements when the LED brightness level was higher than 3. An extra blackout material was also placed above pinhole columns of medium brightness when the LED brightness level was higher than 7 to obtain best data for the faintest pinholes. The ratio of the faintest pinholes to the brightest ones was derived by connecting above ratios, as a final product. The procedure of brightness determination is described in table 13. The brightness ratios of individual columns to the 1st column are tabulated in table 14.

The brightness ratios at different LED currents were determined in the same manner. The results are tabulated in table 15.

Intense photon dose in this life time test was carried out with the new light source at the LED brightness level of 10. Count rate of individual pinholes and corresponding magnitude in terms of B0 star are listed in table 16. The highest illumination was $2\text{E}+6$ c/s (5.6mag B0 star with the clear filter), which was 10 times as bright as that in the previous experiment.

Table 13. Column to column brightness ratios measured at different LED current level

Level	L=10	L=9	L=8	L=7	L=5	L=4	L=3	L=2	L=1
11									110.52
10									110.85
9								17.32	16.65
8								11.87	11.67
7					177.486	10.279	10.094	1.327	1.261
6					155.265	8.866	8.764	1.00*	1.00*
5				18.189	17.820	1.00*	1.00*		
4				9.065	8.885	0.4867			
3		1.807	1.801	1.920	1.807				
2	1.046	1.056	1.047	1.073	1.016				
1	1.00*	1.00*	1.00*	1.00*	1.00*				

Table 14. Brightness ratio among the pinhole columns

column	1	2	3	4	5	6	7	8	9	10	11
Brightness	1.00	1.05	1.80	9.00	18.0	160	183	1900	2700	17700	17700

Table 15. Brightness of LEDs at different current levels

Level	L=1	L=2	L=3	L=4	L=5	L=6	L=7	L=8	L=9	L=10
current	.02	.05	.10	.20	.49	.99	1.98	4.95	9.91	19.8 mA
Intensity	1.00	3.82	11.7	37.1	179	529	1600	6500	15600	31500

Table 16. Pinhole brightness at LED current level = 10

column	1	2	3	4	5	6	7	8	9	10	11
Brightness (c/s)	117	123	210	1050	2100	19k	21k	220k	320k	2070k	2070k
B0 star (mag)	16.2	16.2	15.6	13.8	13.1	10.7	10.6	8.0	7.6	5.6	5.6

Ref-10

Kawakami H. and Fordham J., "Flat Field coincidence loss in the MIC detector for XMM-OM", XMM-OM/MSSL/TC/0050 (1998).

Files used for this section

/depfm8/zpin507.dat

zpin527.dat - zpin537.dat

/depfm8/pincal.dat

11. Measurement

Three F-F images for reference were acquired in photon counting mode before starting the intense photon dose. They were illuminated by the blue LED (460nm) at the light level of 8,000-12,000 c/s/(18x18 mm²). CCD readout window was placed at the right edge of the detector to cover the whole 11x11 pinhole array image. The CCD camera format of 256(H) x100(V) was employed to achieve a fast frame rate, 217Hz. The individual CCD pixels were divided into 8x8 subpixels, which created the plate scale of 1 subpixel = 9.69 μ m.

Pulse height distributions for reference were measured before starting the photon dose. The light source was the pinhole image. This lighting enabled to involve the exactly same pores of MCPs as those of the photon dose. The pulse height distributions were derived separately for the individual pinhole columns, 4-11. The brightest pinholes (column 10 and 11) were covered with the optional blackout material when measuring the pinhole columns 4-7.

The intense photon dose was carried out at the LED brightness level = 10, which provided pinhole illumination of 117 - 2,070,000 counts/sec/pinhole. The exposure time of the photon dose increased day by day, namely 18min for the 1st day, 42min the 2nd, 2 hours 3rd, 4 hours 4th, 8 hours 5th, 15 hours 6th, 20 hours 7th and 8th, and finally 30 hours in the 9th day. The total exposure time reached 100 hours.

Pulse height distributions for the individual columns were measured twice after each photon dose, i.e. within 1.5 hours after the illumination and on the following day.

Fluorescences were monitored with the time resolution of 5min until 30min since the end of illumination. Another series of fluorescence monitoring started later than 1.5 hours since the end of illumination. It continued until the next intense illumination with the time resolution of 2 hours. A 15 hours F-F image was acquired in photon counting mode, starting later than 24 hours since the end of illumination. The light source was the blue LED (460nm) tuned at the light level of 8,000-12,000 c/s/(18x18 mm²). Its integration was carried out in the middle of the fluorescence monitoring, since the fluorescence in the F-F had to be corrected for an accurate analysis. Both of F-F and fluorescence were acquired in photon counting mode with the CCD camera format of 256 (H) x100(V). 800(H)x800(V) pixels, which contains the whole 11x11 pinhole array image, were extracted out of full image, format 2048(H)x800(V) pixels, and were stored into a hard disk.

The detector was illuminated intensively for one minute between two long intense illuminations to gauge the remaining fuel for fluorescence (i.e. impure ions within the MCP pores). The subsequent fluorescences were monitored with time resolution of 5min until 30min since the end of illumination.

F-F images in analog mode, which include effects due to both of photocathode sensitivity loss and MCPs gain depletion, were sometimes measured.

All of experiments carried out are summarized in Appendix.

12. Fluorescence

A strong and long lasted fluorescences appeared after an intense illumination as shown in Fig. 19. This affects F-F images of this experiment, and may do a science data of XMM-OM if the telescope is pointed to a bright star even for a short time.

In order to identify the origin and mechanism of fluorescence, the intensifier was illuminated intensively several times with different photocathode voltages, and the subsequent fluorescences were monitored. The experiment procedures and evidences were;

- i) The intensifier was intensively illuminated for 1 min with photocathode voltage = 0V and with MCPs ON. A dark image was integrated for 5min, starting at 30sec after the end of illumination, with photocathode voltage = 400V and with MCPs ON. No fluorescence was seen in the dark image (Zbin541.dat).
- ii) The intensifier was intensively illuminated for 1 min with photocathode voltage = 400V and with MCPs ON. A dark image was integrated for 5min, starting at 30sec after the end of illumination, with photocathode voltage = 400V and with MCPs ON. A significant fluorescence was seen in the dark image (ZDrk542.dat).
- iii) The intensifier was intensively illuminated for 10 min with photocathode voltage = 400V and with MCPs ON. A dark image was integrated for 5min, starting at 23min after the end of illumination, with photocathode voltage = 400V and with MCPs ON. Fluorescences were seen in the dark image (ZDrk574.dat). Next dark image was integrated for 10min, starting at 32min after the end of illumination, with photocathode voltage = 0V and with MCPs ON. Fluorescence was not seen in the dark image (ZDrk575.dat).

illumination			image acquisition			fluorescence
Vc	Vmcp	exposure	Vc	Vmcp	integration	
i) 0V	2250V	1min	400V	2250V	5min	None
ii) 400V	2250V	1min	400V	2250V	5min	seen
iii) 400V	2250V	10min	400V	2250V	5min	seen
			0V	2250V	10min	None

From the above 3 evidences, it is concluded that the fluorescence is originated in photocathode, which stores electrons generated by ion feedback from MCP pores and emitted slowly. The evidence (iii) ruled out the possibility of glow within MCP pores. The evidence (i) ruled out the possibility of glow at detector window or at photocathode generated by the input photons.

The 11x11 array of fluorescence spots were averaged along the columns to improve S/N. Then, the acquired events within central $D=21$ twixels ($= 407\mu\text{m}$) circular region were summed up to determine whole fluorescence from a spot. Background dark current was determined from 37×37 square twixels ($=717\mu\text{m}$) region excluding the $D=21$ twixels circle, and was subtracted. Figs. 20a-20c show time profiles of fluorescence until 10 hours since the end of illuminations. The count rate was pretty high, 8000 counts/hour/spot, in the first 5min when illuminated for 42 min by the $2\text{E}+6$ c/s pinholes in the 4th day (Fig. 20a). The fluorescence of this short duration component decreased to 1/10 in 1 hour. The short duration component did not depend much on the illumination period. For instance, a 10 min illumination in the 1st day created fluorescence of 3700 counts/hour/spot in the 2nd 5 min, while 4 hours illumination in the 4th day 4100 counts/hour/spot in the 2nd 5 min (Fig. 20b). The fluorescence in the 9th day even faded due to exhaustion of fuel after the 100 hours scrubbing (Fig. 20c).

The fluorescence of short duration component is followed by long duration component (Figs. 21a-21c), which did not emit intensively but remained to emit 100 counts/hour/spot even 1 day after an illumination. This component increased significantly with illumination period as shown in Figs 21a and 21b (42 min and 4 hours illuminations). Further long illumination period of 30 hours, however, did not (Fig. 21c). The fluorescence rather faded due to the lack of fuel.

One minute intense illuminations were carried out between two long illuminations to gauge the remaining fuel. Subsequent fluorescences were monitored for 25min ($5 \times 5\text{min}$). The monitoring was always started at 30 seconds after the 1 min illumination. The 11x11 array of fluorescence spots were averaged along the columns to improve S/N. The day by day change of the averaged spots is shown in Fig. 22. Right hand side of the fluorescence profile disappeared gradually. By this effect, the centre of gravity of the fluorescence, which coincided with pinhole position in the 1st day, shifted toward left by 4 twixels ($= 77.5\mu\text{m}$) in the last day. Fig. 23 shows fluorescence profile at the column 11 ($2\text{E}+6$ c/s illumination) along different days. The fluorescence decreased with the days. Fig. 24 shows fluorescence count rate normalized by that in the 1st day. The figure suggests ion feedback decreased after $1\text{E}+9$ dose events.

Fig. 25 shows the day by day change of the fluorescence profile of the long duration component. The fluorescences were started to be integrated later than 1.5 hours since the end of the long illuminations. The 11x11 array of fluorescence spots were added together along the columns. Since the integration period, start of the integration, and illumination period were different day by day, the absolute intensity of the spots do not have meaning. Therefore, the intensities of fluorescence profile were normalized by the spots at columns 10 and 11 for each day. The poor S/N of the 5th day was due to break down of the MIC electronics for a whole day. The image acquisition re-started at 21 hours since the end of illumination and total integration period was only 6 hours.

The width of fluorescence increased with time. The profile at the columns 8-11 eventually got black hole in the centre. The position of the black hole coincides with the pinhole position. The long duration component showed non-linearity against estimated ion feedback. For instance, the intensities of fluorescence at columns 8 - 9 (220k-320k c/s) are nearly same as those at columns 10 - 11 (2070 kc/s). Within a profile, wing part is enhanced. The short decay component did not show the doughnut shape, mentioned above, since it had not extended wing in profile. Fig. 26 shows profiles of the long and the short duration components after completing the 100 hours photon dose. The difference between the 2 components is clear.

The correction of fluorescence was essential to assess sensitivity loss in a photon counting F-F image in this experiment, even if the F-F was acquired 1 day after illumination. Two adjacent dark images, before and after a F-F, were used for estimating fluorescence in the F-F. Then, the impact on sensitivity loss at peak and average were calculated consulting with the standard profiles shown Fig. 25. The corrections for peak and average were, for instance, 1% at the brightest pinhole positions in the F-F on the 4th day, whose acquisition was started at 26 hours since the end of illumination. The F-F image on the first day was unusual, because its acquisition was carelessly started only 3 hours later the end of illumination. The corrections were 3.7% and 2.6% for peak and average. The correction became smaller in the latter days both for peak and average, because of the exhaustion of fuel.

A dark image was integrated for 5 min, starting at 1 min after an 1min illumination on the 1st day, while the other dark integration was started 30 sec after the other 1min illumination. Impulsive component of the fluorescence was derived by differentiating these 2 dark images. Fluorescence from the $2E+6$ c/s pinholes were 375 counts/spot during the elapsed time of 0.5-5.5 min since the end of illumination, 300 counts/spot during 1.0-6.0 min, and 12 counts/spot during 5.5-6.0 min. These led that fluorescence of 87 counts/spot (10000 c/hour/spot) was emitted during the impulsive period, 0.5-1.0 min.

The 1min intense illuminations were followed by a 2min and a 10min illuminations in the 1st day to investigate the dependence of fluorescence on illumination period. The fluorescence in the 1st 5min after the 1 min illumination was 56% of that after the 10min illumination for the $2E+6$ c/s pinholes, and the 2 min illumination was 75%. It is extrapolated that a 10sec illumination by $2E+6$ c/s pinholes causes fluorescence of 95 counts in the 1st 5min. Therefore, it is safer not starting observation for more than 5min if 5.6mag star is accidentally captured by the OM-telescope.

No fluorescence was detected after 30 hours illumination with the intensity of 2.1 kc/sec/pinhole (13.1mag B0 star). A little fluorescence was, however, seen in the long duration component after 4 hours illumination with the intensity of 19 kc/sec/pinhole (10.7mag B0 star).

Ref-12 Files used for this section
/depfm8/Zbin541.dat

ZDrk542.dat - ZDrk575.dat
ZDrk579.dat, ZDrk581.dat, ZDrk584.dat
ZDrk588.dat - ZDrk592.dat
ZDrk594.dat - ZDrk596.dat
ZDrk599.dat, ZDrk601.dat
ZDrk602.dat - ZDrk606.dat
ZDrk611.dat - ZDrk619.dat
ZDrk622.dat, ZDrk624.dat
ZDrk625.dat - ZDrk629.dat
ZDrk631.dat - ZDrk641.dat, ZDrk644.dat
ZDrk645.dat - ZDrk663.dat
ZDrk665.dat, ZDrk667.dat, ZDrk669.dat, ZDrk670.dat,
ZDrk671.dat - ZDrk675.dat
ZDrk678.dat - ZDrk684.dat
ZDrk686.dat - ZDrk695.dat
ZDrk697.dat - ZDrk699.dat, ZDrk701.dat
ZDrk702.dat - ZDrk706.dat
ZDrk709.dat - ZDrk713.dat
ZDrk715.dat - ZDrk727.dat
ZDrk729.dat, ZDrk730.dat, ZDrk732.dat, ZDrk734.dat,
ZDrk735.dat - ZDrk740.dat
ZDrk744.dat - ZDrk749.dat
ZDrk751.dat - ZDrk753.dat, ZDrk755.dat, ZDrk757.dat
ZDrk759.dat - ZDrk763.dat
ZDrk767.dat - ZDrk772.dat
ZDrk773.dat - ZDrk777.dat
ZDrk779.dat - ZDrk789.dat
ZDrk792.dat, ZDrk794.dat, ZDrk795.dat
ZDrk797.dat - ZDrk799.dat
ZDrk801.dat, ZDrk803.dat, ZDrk808.dat
ZDrk811.dat - ZDrk815.dat
ZDrk817.dat - ZDrk819.dat, ZDrk821.dat, ZDrk822.dat
ZDrk824.dat - ZDrk839.dat
ZDrk841.dat - ZDrk843.dat
ZDrk846.dat - ZDrk848.dat
ZDrk851.dat, ZDrk852.dat
ZDrk855.dat - ZDrk863.dat
ZDrk867.dat - ZDrk871.dat
ZDrk874.dat - ZDrk878.dat, ZDrk880.dat

13. Gain depletion of MCPs

Pulse height distributions (hereafter, PHD) for individual columns, 4-11 ($2E+3$ - $2E+6$ c/s), in the pinhole array were measured twice after each photon dose, i.e. within 1.5 hours after the illumination and on the following day. The recovery on the following days was significant in the earlier days for the weaker illumination. Pulse height distribution was also monitored for half month after completing this photon dose test. Recoveries of 3-5% were seen.

Fig. 27a shows the original PHD before the dose and the one after 100 hours photon dose by the $2E+6$ c/s pinholes. The gain reduced to 1/3 of the original. Fig. 27b shows the same PHDs, but the one after the 100 hours dose was expanded along abscissa for comparison. Wing profile in high energy side of the expanded PHD looks similar to the non-dosed PHD, but valley in the lower energy side disappeared. The gain depletions throughout this experiment were quantified from peak positions of the PHDs. The peak shape of the PHD, however, became fuzzy if the gain depletion was too strong as shown in the figure. Therefore, the gain depletion was determined manually by looking at wing in high energy side, when the gain was lower than 0.4 of the original.

Day by day change of MCP gain is tabulated in Table 17. The results are plotted against integrated dose events as shown in Fig. 28. The gain decreased more slowly for the higher intensity pinholes. This is due to pore paralysis of MCPs. It will be helpful for modelling if the gain depletion could be plotted against accumulated anode current, instead of accumulated dose events (ref. James(1998)).

The threshold level for event detection in the photon counting imaging was modified from 30ADU to 15ADU during XMM-OM project. This experiment employed threshold level of 15ADU for most of image acquisition. This change rescued many photons, which were supposed to be lost after the severe gain depletion in the former threshold level. The last 7 F-F images were acquired in even lower threshold level, 8ADU, to separate photocathode sensitivity loss more clearly from the effect of gain depletion. The event losses due to the gain depletion were calculated with the both threshold levels, 15ADU and 8ADU, and were tabulated in Table 18.

The gain depletion for DEP's QM-intensifier was plotted in the same scale in Fig. 29. It did not contain very high intensity illumination ($2E+6$ c/s), but medium to low intensity illuminations showed that the QM-intensifier decreased gain more slowly by 50%.

Table 17. Gain depletion (fitted by hand, if gain < 0.4)

Total dose (hour)		Pinhole intensity (counts/sec)							
		1.1k	2.1k	19k	21k	220k	320k	2070k	2070k
0.3	I,*	.918,	.947,	.957,	.949,	.922,	.908,	.855,	.836,
0.3	D,*	.999,	.971,	.977,	.968,	.927,	.922,	.847,	.854,
1.0	I,	.978,	.968,	.943,	.928,	.872,	.850,	.751,	.765,
1.0	D,	.997,	.993,	.973,	.964,	.875,	.874,	.774,	.785,
3.0	I,	.954,	.946,	.885,	.894,	.779,	.756,	.662,	.663,
3.0	D,	.999,	.965,	.925,	.925,	.815,	.783,	.685,	.687,
7.0	I,	.952,	.902,	.842,	.844,	.726,	.694,	.572,	.567,
7.0	D,	.930,	.917,	.835,	.854,	.721,	.677,	.572,	.581,
15.0	D,	.875,	.847,	.741,	.741,	.638,	.609,	.452,	.493,
30.0	I,	.908,	.878,	.713,	.705,	.522,	.501,	.392,	.408,
30.0	D,	.884,	.869,	.718,	.718,	.540,	.510,	.408,	.408,
50.0	I,	.870,	.837,	.636,	.649,	.465,	.439,	.317,	.345,
50.0	D,	.889,	.853,	.674,	.671,	.500,	.465,	.339,	.351,
70.0	I,	.826,	.793,	.588,	.586,	.400,	.385,	.260,	.278,
70.0	D,	.840,	.826,	.606,	.609,	.435,	.400,	.286,	.299,
100.0	I,	.825,	.768,	.540,	.541,	.351,	.347,	.238,	.238,
100.0	D,	.836,	.800,	.590,	.585,	.385,	.357,	.238,	.250,
100.0	3D,	.832,	.797,	.591,	.584,	.385,	.370,	.250,	.270,
100.0	4D,	.858,	.823,	.611,	.610,	.408,	.392,	.263,	.286,
100.0	5D,	.867,	.833,	.618,	.613,	.417,	.392,	.278,	.290,
100.0	8D,	.848,	.802,	.585,	.595,	.417,	.385,	.278,	.286,
100.0	10D,	.861,	.827,	.622,	.621,	.435,	.426,	.294,	.294,
100.0	11D,	.871,	.827,	.629,	.646,	.435,	.412,	.294,	.303,
100.0	15D,	.862,	.828,	.642,	.639,	.435,	.417,	.303,	.308,
100.0	17D,	.874,	.847,	.630,	.629,	.444,	.426,	.290,	.303,
100.0	19D,	.866,	.820,	.643,	.641,	.455,	.417,	.294,	.313,

Note) I: PHD was measured Immediately after intense illumination
 xD: PHD was measured x Days after intense illumination

Table 18. Sensitivity loss due to gain depletion

Total dose (hour)	Pinhole intensity (counts/sec)									
	120c/s	210	1.1k	2.1k	19k	21k	220k	320k	2070k	2070k
(Threshold = 15 ADU)										
0.3	.000	.000	.000	.002	.001	.002	.004	.005	.007	.009
1.0	.000	.000	.000	.000	.002	.002	.007	.009	.012	.013
3.0	.000	.000	.000	.002	.005	.005	.011	.017	.018	.020
7.0	.000	.000	.006	.006	.010	.010	.018	.027	.030	.031
15.0	.000	.000	.010	.012	.016	.019	.026	.036	.054	.048
30.0	.000	.000	.009	.010	.018	.021	.039	.053	.068	.073
50.0	.000	.000	.008	.011	.022	.025	.047	.063	.099	.098
70.0	.000	.000	.012	.014	.030	.033	.065	.086	.140	.134
100.0 1D	.000	.000	.013	.016	.032	.036	.083	.105	.195	.186
100.0 3D	.000	.000	.013	.016	.032	.036	.083	.099	.180	.162
100.0 4D	.000	.000	.011	.014	.029	.032	.073	.088	.163	.145
100.0 5D	.000	.000	.010	.013	.028	.032	.070	.088	.148	.142
100.0 8D	.000	.000	.012	.016	.032	.035	.070	.092	.148	.145
(Threshold = 8 ADU)										
100.0 8D	.000	.000	.000	.000	.000	.000	.015	.023	.037	.039
100.0 10D	.000	.000	.000	.000	.000	.000	.012	.016	.033	.036
100.0 11D	.000	.000	.000	.000	.000	.000	.012	.019	.033	.033
100.0 15D	.000	.000	.000	.000	.000	.000	.012	.018	.030	.032
100.0 17D	.000	.000	.000	.000	.000	.000	.011	.016	.034	.033
100.0 19D	.000	.000	.000	.000	.000	.000	.010	.018	.033	.031

Ref-13

James A. "A fast plasma analyser for the study of solar wind interaction with Mars",
PHD thesis for UCL (1998).

Files used for this section

/depfm8/ZPHD539.dat

ZPHD578.dat, ZPHD582.dat, ZPHD593.dat, ZPHD597.dat
 ZPHD607.dat, ZPHD620.dat, ZPHD630.dat, ZPHD642.dat
 ZPHD664.dat, ZPHD685.dat, ZPHD696.dat
 ZPHD714.dat, ZPHD728.dat, ZPHD750.dat, ZPHD754.dat
 ZPHD778.dat, ZPHD790.dat, ZPHD800.dat, ZPHD804.dat
 ZPHD809.dat, ZPHD823.dat, ZPHD844.dat, ZPHD849.dat
 ZPHD864.dat, ZPHD872.dat, ZPHD882.dat

14. Sensitivity loss in photon counting image

A F-F image with the blue LED (460nm) was integrated for 15 hours in photon counting mode after each intense illumination to see the impact on science image. The integration started at the elapsed time of >24 hours after the illuminations (except in the 1st day) to avoid fluorescence. Fig. 30 shows 2 raw F-F images, one taken prior to the photon dose for reference and the other after the 100 hours dose. The F-F after the dose clearly shows an array of black spots corresponding to the pinhole positions.

A F-F image in each day of photon dose was divided by the reference F-F to remove detector artefacts and illumination non-uniformity. Then, the 11x11 array of black spots were averaged along the columns to improve S/N. Central positions of the black spots coincided with pinhole positions in the accuracy of 10 μ m. The day by day growth of the black spots is shown in Fig. 31. These images contain all factors, i.e. fluorescence, gain depletion and photocathode sensitivity loss. White spots appeared at 2E+6 c/s pinhole positions in the 1st day, as the fluorescence dominated photocathode sensitivity loss and MCPs gain depletion. The black spots are seen for the illumination intensities of > 19kc/s after the 100 hours dose but not obvious for the illumination intensities of < 2.1kc/s. This is big improvement from the DEP-QM intensifier, in which black spots were clearly seen for the illumination intensities of 0.8kc/s after 21 hours dose (ref. XMM-OM/MSSL/TC/0044). Fig. 32 shows profiles of the averaged black spots from the 5th to the 9th days. Y-width of the slice is 3 twixel (= 58 μ m). Since the integrations were started after the decay of fluorescence for these 5 F-Fs, the peak depths were not affected by fluorescence more than 0.8%. The depth of black spots reached 30% for the brightest illumination after 100 hours dose.

The sensitivity loss at the peak position was quantified from the average of 3x3 twixels square centred on the black spots. The normalization level was determined from 37x37 twixels (=717 μ m) square excluding central D=21 twixels circular area. Then, the effect of fluorescence (3.8% in maximum) was subtracted. The results were tabulated in Table 19 and were plotted against accumulated dose events in Fig. 33. The sensitivity did not decrease up to 1E+8 dose events. It started to decrease steeply from 1E+10 dose events. The sensitivity decreased more slowly for the brighter pinholes. This is again the effect of pore paralysis.

The sensitivity loss for DEP's QM-intensifier was plotted in the same frame as shown in Fig. 34. The QM-intensifier lost sensitivity by 3% at 3E+7 dose events, while the DEP_#8 intensifier did not up to 3E+9 dose events. The ruggedness of DEP_#8 intensifier is clear at the lower dose events.

The sensitivity loss in F-F image was averaged over central D=210 μ m (=11 twixels) circular area to characterize spatial extent of damage as well as the depth. The results are tabulated in Table 20 and plotted in Fig. 35 after the correction of fluorescence.

A Gaussian profile was fitted to deep black spots to investigate the spatial extent directly. The results are tabulated in Table 21 and shown in Fig. 36. The width of the black spots increased with accumulated dose events. It started from 80 μ m(FWHM) and reached 120 μ m after acquiring 1E+12 dose events.

The sensitivity loss seen in F-F image is the combination of gain depletion and photocathode sensitivity loss. The photocathode sensitivity losses were calculated by removing the effect of gain depletion. The results were tabulated in Table 22 and were shown in Fig. 37. The sensitivity loss of photocathode is not obvious up to 1E+9 dose events. The plot has large scatter at larger dose events, since the calculation becomes less accurate when the gain depletion is large. For instance, 20% of photo-events were lost due to the gain depletion at 2E+6 c/s pinhole position after 100 hours dose.

Table 19. Sensitivity decrease in blue F-F at peak

Total dose (hour)	Pinhole intensity (counts/sec)									
	120c/s	210	1.1k	2.1k	19k	21k	220k	320k	2070k	2070k
0.3	.996	1.004	.989	1.000	.996	.991	.994	.984	.979	.981
1.0	.994	.980	.990	.983	.986	.992	.999	.988	.980	.983
3.0	.997	1.003	.996	1.000	.983	.986	.981	.967	.968	.971
7.0	.997	1.002	.998	1.012	.971	.981	.963	.961	.911	.928
15.0	.998	.995	.984	1.000	.970	.975	.934	.937	.870	.894
30.0	.999	1.002	.988	1.001	.954	.960	.905	.896	.785	.821
50.0	.994	.992	.984	.990	.942	.950	.883	.878	.747	.779
70.0	1.009	.996	.979	.990	.929	.917	.844	.836	.667	.694
100.0 1D	.996	1.000	.974	.979	.932	.925	.824	.819	.623	.665
100.0 2D	1.003	.980	.976	.981	.942	.938	.881	.848	.652	.698
100.0 5D	1.001	.990	.979	.981	.948	.944	.879	.852	.663	.713

Table 20. Sensitivity decrease in blue F-F averaged over D=213um circular area

Total dose (hour)	Pinhole intensity (counts/sec)									
	120c/s	210	1.1k	2.1k	19k	21k	220k	320k	2070k	2070k
0.3	.996	.999	1.001	.997	.998	1.000	.996	.994	.992	.989
1.0	.998	1.001	1.000	.998	.995	.994	.995	.989	.991	.991
3.0	.998	.998	1.000	1.000	.997	.998	.994	.989	.993	.988
7.0	.997	.997	1.004	1.000	.997	.994	.989	.983	.972	.973
15.0	.996	.994	1.002	.999	.996	.992	.980	.974	.956	.952
30.0	.995	.994	1.004	.998	.987	.988	.968	.958	.925	.924
50.0	.994	.995	1.000	.995	.983	.986	.959	.952	.906	.906
70.0	1.000	.990	.999	.992	.980	.976	.946	.939	.872	.875
100.0 1D	.996	.995	.999	.992	.974	.975	.934	.925	.846	.846
100.0 2D	.997	.993	1.000	.993	.980	.978	.942	.930	.855	.858
100.0 5D	.997	.994	.999	.996	.983	.984	.948	.938	.868	.874

Table 21. Gaussian width of depletion profile in blue F-F (FWHM, um)

Total dose (hour)	Pinhole intensity (counts/sec)									
	120c/s	210	1.1k	2.1k	19k	21k	220k	320k	2070k	2070k
0.3	N/A	N/A	N/A	N/A	N/A	N/A	N/A	N/A	N/A	N/A
1.0	N/A	N/A	N/A	N/A	N/A	N/A	N/A	N/A	N/A	N/A
3.0	N/A	N/A	N/A	N/A	N/A	N/A	87.6	85.2	75.8	59.3
7.0	N/A	N/A	N/A	N/A	N/A	N/A	83.6	91.0	91.8	84.1
15.0	N/A	N/A	N/A	N/A	N/A	N/A	92.0	106.0	101.0	97.7
30.0	N/A	N/A	N/A	N/A	N/A	N/A	95.3	104.1	111.8	104.9
50.0	N/A	N/A	N/A	N/A	N/A	N/A	102.2	106.5	117.0	113.2
70.0	N/A	N/A	N/A	54.4	88.9	85.8	109.9	110.8	123.8	114.5
100.0 1D	N/A	N/A	45.7	83.1	90.1	112.7	103.2	111.5	122.1	122.8
100.0 2D	N/A	N/A	58.7	88.0	79.5	105.3	105.1	111.0	124.2	121.0
100.0 5D	N/A	N/A	55.8	129.2	77.2	101.0	103.6	112.3	124.3	118.1

Table 22. Photocathode sensitivity decrease at peak

Total dose (hour)	Pinhole intensity (counts/sec)									
	120c/s	210	1.1k	2.1k	19k	21k	220k	320k	2070k	2070k
0.3	.996	1.004	.989	1.002	.997	.993	.998	.989	.986	.989
1.0	.994	.980	.990	.983	.988	.994	1.006	.997	.992	.996
1.0	.994	.980	.990	.983	.988	.994	1.006	.997	.992	.996
3.0	.997	1.003	.996	1.002	.988	.991	.992	.984	.986	.991
7.0	.997	1.002	1.004	1.018	.981	.991	.981	.988	.939	.958
15.0	.998	.995	.994	1.012	.986	.994	.959	.972	.920	.939
30.0	.999	1.002	.997	1.011	.972	.980	.942	.946	.842	.885
50.0	.994	.992	.992	1.001	.963	.975	.926	.937	.829	.864
70.0	1.009	.996	.991	1.004	.958	.948	.903	.915	.776	.801
100.0 1D	.996	1.000	.986	.995	.963	.959	.899	.915	.774	.817
100.0 2D	1.003	.980	.989	.997	.973	.973	.961	.942	.795	.833
100.0 5D	1.001	.990	.989	.994	.975	.975	.945	.934	.778	.831

Ref-14

Kawakami H. "The DEP chevron image intensifier tube", XMM-OM/MSSL/TC/0044 (1997).

Files used for this section

/depfm8/ZDEP580.dat, ZDEP600.dat, ZDEP623.dat, ZDEP643, ZDEP668
ZDEP700.dat, ZDEP733.dat, ZDEP756.dat
ZDEP793.dat, ZDEP796.dat, ZDEP810.dat

15. Photocathode sensitivity loss at different colours

After completing the 100 hours photon dose, F-F images with red and green LEDs were acquired in photon counting mode to assess colour dependence of photocathode damage. The gain depletion of MCPs for the >320 kc/s illumination was very severe at 1 day after the illumination, and was dominant cause of sensitivity loss (10-20%) in the F-F images. Fortunately, the gain recovered slowly in a week, and lightened the effect on the F-Fs. All F-Fs analyzed in this section were acquired later than 5 days after completing the 100 hours dose. These F-Fs were free from fluorescence, as the elapsed times were sufficiently long.

The 11×11 array of black spots in the F-F images were averaged along the columns (Fig. 38). Fig. 39 shows the slices of the black spots in the three colours. Both of depth and width are largest in red. Although the gain depletion was still recovering very slowly, these profiles should be very close to permanent sensitivity loss.

Fig. 40 shows sensitivity loss at depletion peak in the blue, green and red F-F images. Fig. 41 shows sensitivity loss averaged over $D=210\mu\text{m}$ circular area. Figs. 42 shows widths of the black spots in the F-F images. These results are tabulated in Tables 23, 24 and 25. It should be noted that the sensitivities must have decreased more slowly for the brighter pinholes due to pore paralysis, but they are not visible in these figures. The sensitivity loss is more severe in the longer wavelength. The loss at peak reached 46% in red for the brightest pinholes, while 36% in green and 32% in blue. The colour dependence of spot width is also clear. The growth of width is largest in red covering 50-195 μm (FWHM), while 50-125 μm in blue (see Fig.36).

It is necessary to remove the effect of gain depletion to estimate the photocathode sensitivity loss from a F-F image. To improve the estimation accuracy, F-F images were acquired with threshold level of 8 ADU in stead of the standard 15 ADU. This reduces the effect of the gain depletion on photon counting images (Table 18), although it might have sacrificed centroiding accuracy and picked up low energy noise events. Since F-F images in the 3 colours were acquired later than 10 days after end of the 100 hours dose, the effects of fluorescence were negligible. The detector was illuminated for one minutes for the fuel test at 8 days after the dose, but it did not affect the F-F images by fluorescence as the illumination period was short.

The 11×11 array of black spots in the F-F images were averaged along the columns (Fig. 38). Fig. 43 shows the slices of the black spots in the three colours. Since effects of gain depletion on the photon counting images were less than 4% even for the highest illumination position, the depth and profile of the black spots approximately show photocathode damage. Then, the sensitivity losses at peak in the 3 colours were estimated by removing the tiny effect of gain depletion, and were plotted in Fig. 44 and tabulated in Table 26. The widths of the black spots are plotted in Fig. 45 and tabulated in Table 27. The photocathode sensitivity loss at peak reached 36% in red for the brightest pinholes, while 27% in green and 20% in blue. The colour dependence of spot width is again clear. Width of photocathode damage is slightly broader than that in F-F image, but almost same. The width at the highest illumination position is 210 μm (FWHM) for red light, while 130 μm for blue. The photocathode damage is more sever in

the longer wavelength.

Table 23. Sensitivity decrease in F-Fs at peak

Total dose (hour)	Pinhole intensity (counts/sec)									
	120c/s	210	1.1k	2.1k	19k	21k	220k	320k	2070k	2070k
Blue										
100.0 hr	1.002	.993	.979	.983	.951	.945	.876	.850	.657	.698
Green										
100.0 hr	.995	1.002	.981	.991	.930	.933	.836	.825	.629	.655
Red										
100.0 hr	.999	.988	.975	.975	.943	.936	.832	.807	.530	.550

Table 24. Sensitivity decrease in F-Fs averaged over D=210um circular area

Total dose (hour)	Pinhole intensity (counts/sec)									
	120c/s	210	1.1k	2.1k	19k	21k	220k	320k	2070k	2070k
Blue										
100.0 hr	.998	.997	.999	.998	.985	.983	.946	.937	.865	.864
Green										
100.0 hr	.999	.997	.999	.996	.976	.980	.937	.928	.832	.830
Red										
100.0 hr	.996	.997	1.000	.994	.979	.975	.915	.908	.738	.729

Table 25. Gaussian width of depletion profile in F-Fs (FWHM, um)

Total dose (hour)	Pinhole intensity (counts/sec)									
	120c/s	210	1.1k	2.1k	19k	21k	220k	320k	2070k	2070k
Blue										
100.0 hr	N/A	N/A	52.7	137.7	72.8	98.8	104.5	114.7	126.3	122.3
Green										
100.0 hr	N/A	N/A	52.0	114.1	96.0	104.8	111.6	117.2	146.7	147.8
Red										
100.0 hr	N/A	N/A	53.0	95.9	88.2	106.8	135.3	145.6	195.7	194.6

Table 26. Photocathode sensitivity decrease at peak after 100 hours dose

Total dose (hour)	Pinhole intensity (counts/sec)									
	120c/s	210	1.1k	2.1k	19k	21k	220k	320k	2070k	2070k
Blue										
100.0 hr	.992	1.002	.984	.998	.954	.947	.897	.897	.756	.807
100.0 hr	.990	.998	.971	.984	.950	.952	.899	.913	.781	.842
100.0 hr	1.003	.990	.982	.996	.968	.964	.931	.929	.754	.831
Green										
100.0 hr	.988	.998	.980	1.000	.951	.947	.879	.891	.696	.763
Red										
100.0 hr	.991	.996	.982	.993	.939	.951	.852	.865	.598	.657
100.0 hr	.996	.990	.981	.961	.957	.947	.896	.891	.591	.667
100.0 hr	.992	.998	.986	.998	.952	.949	.870	.874	.623	.680

Table 27. Gaussian width at photocathode damage (FWHM, um) after 100 hours dose

Total dose (hour)	Pinhole intensity (counts/sec)									
	120c/s	210	1.1k	2.1k	19k	21k	220k	320k	2070k	2070k
Blue										
100.0 hr	N/A	N/A	N/A	N/A	81.6	104.7	104.7	107.1	128.0	128.4
100.0 hr	N/A	N/A	N/A	N/A	93.5	109.7	116.4	113.7	126.6	135.2
100.0 hr	N/A	N/A	N/A	N/A	58.5	101.7	99.3	118.7	133.4	133.6
Green										
100.0 hr	N/A	N/A	N/A	N/A	78.8	106.3	109.1	112.0	148.2	156.1
Red										
100.0 hr	N/A	N/A	N/A	N/A	79.1	114.1	143.3	144.5	205.1	205.5
100.0 hr	N/A	N/A	N/A	N/A	83.6	112.1	157.5	149.6	215.8	216.8
100.0 hr	N/A	N/A	N/A	N/A	79.6	127.4	150.8	145.7	205.8	208.0

Ref-15 Files used for this section

/depfm8/ZDEP810.dat, ZDEP816.dat, ZDEP820.dat (TH=15 ADU)

ZDEP845.dat, ZDEP850.dat, ZDEP854.dat (TH= 8 ADU)

ZDEP866.dat, ZDEP873.dat, ZDEP879.dat (TH= 8 ADU)

16. Spatial extent of MCPs gain depletion

A F-F image in analog mode includes effects due to both of photocathode sensitivity loss and MCP gain depletion, while a F-F image in photon counting mode mainly effect due to phtocathode and a little due to gain depletion. The effect of gain depletion was extracted from the analog F-F by comparing with the photon counting F-F.

Fig. 46 shows a F-F image acquired in analog mode with the comparison of that in photon counting mode. Both F-Fs were illuminated by the blue LED, since the photocathode damage was smallest in blue among the 3 colours. The threshold level was set to 8ADU for the photon counting imaging to highlight the photocathode damage, in which the estimated photon loss due to the gain depletion is only 3% for the highest dose positions. The photon counting F-F image was binned by 8x8 to match the plate scale to that of the analog F-F. The sliced profile along the highest dose spots shows sharp depletion at the pinhole position in the photon counting F-F. The profile in the analog F-F shows a large extent of depleted region as well as the sharp depletion. The width of the sharp depletion is a little broader in analog image, but it is due to image blurring by under sampling of a CCD pixel and spatial extent of event splash on the phosphor screen.

Fig. 47 shows the analog F-F divided by the photon counting F-F. Since sensitivity loss in the photon counting F-F is mainly due to phtocathode damage, the figure approximately describes spatial distribution of MCP gain depletion. It shows plateau at the depth of 35%, bridging black spots. The black spots are still seen in the 2 dimensional image but their depths are not significant. Fig. 48 is the magnified image. A sliced profile shows that the extent of the gain depletion for the highest dose spots is 800um (half width at half depth). The spatial extent of gain depletion was discovered by Edgar et. al. in 1992 (Ref-16). This experiment showed similar extent of gain depletion.

Depth of the depletion in the analog F-F is not consistent with the gain depletion derived from pulse height distribution. The gain depletions were 30% from the analog F-F, while 65% from the pulse height distribution. Illumination for PHD was the pinhole images in a modest count rate (30-50 c/s/pinhole). The possibility of pore paralysis is ruled out, because the pulse height distributions by pinhole illumination and by F-F illumination were same before starting the photon dose.

One of the explanation is large gain drop (~ 45%) at MCP1. When illuminated by the pinholes, all photo-electrons fall into specific pores of MCP1 (diameter~70um). While, when illuminated by a F-F, event splash, which came through other MCP1 pores outside the 70um diameter, can hit the CCD pixel located beneath a black spot, because of the wide spread of event splash and under sampling of a CCD pixel. The full width of this image blurring is about 100um, which can dilute the deep and sharp gain depletion at the pinhole positions. A shallow gain depletion is ideal for the 10 years XMM-OM observations even if damage area is large. When the gain depletion region covers whole detector field evenly, it can be compensated by raising HVs to MCPs. This hypothesis on the gain depletion at MCP1 suggests deep and sharp damage, which is not ideal for the XMM-OM.

Ref-16

Edgar M., Lapington J. and Smith A. "The spatial extent of gain depression for MCP-based photon detectors", Rev. Sci Instrum vol 63 p816 (1992).

Files used for this section

/depfm8/ZAna865.dat, ZDEP866.dat

17. Summary

a) There are short duration (<30min) and long duration components in fluorescence. One minute illumination by a 5.6mag B0 star (2070 kc/sec/pinhole) caused fluorescence of 330 counts in the 1st 5min. It is extrapolated that a 10sec illumination can cause fluorescence of 95 counts in the 1st 5min. No fluorescence was detected after 30 hours illumination by a 13.1mag star (2.1 kc/sec/pinhole). A little fluorescence was, however, seen in the long duration component after 4 hours illumination by a 10.7mag star (19 kc/sec/pinhole).

The long duration component was not intense but lasted more than 1 day. For instance, fluorescence was still 80counts/hour/spot one days after 42min illumination by the 5.6mag star.

Longer illumination was not effective to increase the short duration component. For instance, 2 hours illumination caused only 700 counts in the 1st 5min. While, it was effective for the long duration component.

Profile of the long duration component is broader than that of short duration component. Exhaustion of fuel for fluorescence was seen after acquiring $1\text{E}+10$ dose events. The profile of fluorescence changed with photon dose. It got doughnut shape after acquiring $2\text{E}+11$ dose events.

b) MCPs gain reduced to half after acquiring $5\text{E}+10$ dose events from a 220 kc/s pinhole (8.0mag B0 star). This life time is shorter than DEP-QM tube by 50%. The gain depletion curve showed 3 branches, depending on the intensity of illumination. This is due to the effect of pore paralysis. It is useful to measure anode current during the intense illumination for modelling the gain depletion.

c) Sensitivity loss was not detected below $1\text{E}+8$ dose events in photon counting image for blue light. The loss became 10% at $3\text{E}+10$ dose events, and reached 35% at $7.5\text{E}+11$ dose events. The improvement in DEP_#8 intensifier is noticeable below $1\text{E}+9$ dose events, compared with DEP-QM intensifier.

d) Photocathode sensitivity loss was not detected below $1\text{E}+9$ dose events for blue light.

e) Width of black spot in a photon counting image increased with photon dose, from 70 to 120um for blue light.

f) The photocathode sensitivity losses were assessed at 3 colours (i.e. 4600, 5500, 6200Å) after completing the 100 hours photon dose. The loss was deeper in the longer wavelength. The width of the black spot was larger in the longer wavelength (200um for red).

It is essential to measure the sensitivity losses in other wavelengths, since the spectral coverage of XMM-OM is 1700-6000Å.

g) Spatial extent of MCP gain depletion, 800um, was seen. It can be assessed more accurately with UV light, where photocathode sensitivity loss is expected to be minimum.

The depth of gain depletion seen in an analog F-F did not agree with the results from pulse height distribution. The inconsistency should be investigated further. Measuring

pulse height distribution with re-positioning pinhole by 60um may give further information.

Appendix. Experiment procedure for DEP_#8 intensifier

17 Sept - 10 Nov 1999

File Name	Pinhole	PHD	Dark	F-F	Time(start)
Before damage for reference					
					1999/09/17
PHD369		1000FR			17H 33M 31S
PHD370	8x8	80000FR			17H 59M 11S
					1999/09/18
Bin371			th=24	54000S	17H 22M 03S
					1999/09/19
Bin372		SW-on	Th=24	54000S	12H 24M 43S
					1999/09/20
DRK373			3600S		12H 56M 40S
ANA374				1000FR	16H 15M 18S
ANA375				200FRs	16H 37M 07S
ANA376			off_cover	200FRs	16H 50M 31S
ANA377			off_cover	200FRs	16H 56M 44S
ANA378			open box	200FRs	17H 07M 03S
ANA379			open box	200FRs	17H 15M 11S
ANA380			op box-sm	200FRs	17H 23M 59S
ANA381			op box-sm	200FRs	17H 29M 16S
ANA382			op v sml	200FRs	17H 38M 55S
ANA383			op v sml	200FRs	17H 46M 11S
ANA384			op v sml	200FRs	17H 51M 37S
Bin385			Th=24	1800S	18H 41M 39S
Bin386			SW-on	Th=24 54000S	19H 17M 49S
					1999/09/21
Bin387			Th=24	3600S	10H 34M 35S
Ana388				4000FRs	12H 58M 46S
DEP389	Res 0600S	630nm			15H 41M 42S
DEP390	Res 0600S				15H 54M 21S
DEP391	Res 0600S				16H 05M 46S
DEP392	Res 0600S				16H 16M 59S
DEP393	Res 0600S				16H 35M 48S
DEP394	Res 0600S	460nm			17H 18M 09S
DEP395	Res 0600S				17H 29M 36S
DEP396	Res 0600S				17H 41M 58S
DEP397	Res 0600S				17H 55M 30S
DEP398	Res 0600S				18H 07M 20S
Bin399			-90R	Th=24 54000S	19H 17M 15S
					1999/09/22
SNP400			Hot spot	4FRs	14H 20M 00S
Bin401			Hot spot	60S	14H 24M 44S
Bin402			Hot spot	60S	14H 30M 22S
SIB403		100FRs x3 mag			16H 15M 00S
SIB502		100FRs x3 mag			16H 40M 00S
Bin504			th=24	54000S	19H 00M 25S
					1999/09/23
FSh505			Flash	50000FRs	11H 35M 18S
PHD506	8x8	80000FR			19H 10M 36S
					1999/09/24
Pin507	L=1	3541S			16H 18M 50S

File Name	Pinhole	PHD	Dark	F-F	Time(start)
\\/\	1min	1st	Day-1	15:32 - 15:33	1999/09/30
Drk542			0300S		15H 33M 41S
Drk543			0300S		15H 40M 26S
Drk544			0300S		15H 46M 44S
Drk545			0300S		15H 53M 05S
Drk546			0300S		15H 59M 36S
\\/\	1min	2nd	Day-1	16:06 - 16:07	1999/09/30
Drk547			0300S		16H 07M 39S
Drk548			0300S		16H 13M 34S
Drk549			0300S		16H 19M 23S
Drk550			0300S		16H 25M 17S
Drk551			0300S		16H 31M 02S
\\/\	1min	3rd	Day-1	16:43 - 16:44	1999/09/30
Drk552			0300S		16H 45M 08S
Drk553			0300S		16H 50M 59S
Drk554			0300S		16H 57M 05S
Drk555			0300S		17H 03M 11S
Drk556			0300S		17H 09M 02S
\\/\	1min	4th	Day-1	17:15 - 17:16	1999/09/30
Drk557			0300S		17H 17M 09S
Drk558			0300S		17H 23M 02S
Drk559			0300S		17H 28M 50S
Drk560			0300S		17H 34M 28S
Drk561			0300S		17H 40M 08S
\\/\	2min	1st	Day-1	17:46 - 17:48	1999/09/30
Drk562			0300S		17H 49M 11S
Drk563			0300S		17H 54M 51S
Drk564			0300S		18H 00M 29S
Drk565			0300S		18H 06M 18S
Drk566			0300S		18H 12M 00S
\\/\	2min	2nd	Day-1	18:18 - 18:20	1999/09/30
Drk567			0300S		18H 21M 09S
Drk568			0300S		18H 26M 47S
Drk569			0300S		18H 32M 27S
\\/\	10min		Day-1	18:40 - 18:50	1999/09/30

[illegible]

[illegible]

File Name	Pinhole	PHD	Dark	F-F	Time(start)
Drk650	-----		0300S		21H 24M 45S
Drk651			0300S		21H 30M 07S
Drk652			0300S		21H 35M 29S
Drk653			0300S		21H 40M 50S
Drk654			0300S		21H 46M 11S
Drk655			7200S		21H 51M 33S
Drk656			7200S		23H 51M 55S
X-LUT broken					1999/10/10
Drk657			7200S		01H 52M 17S
Drk658			7200S		03H 52M 39S
Drk659			7200S		05H 53M 01S
Drk660			7200S		07H 53M 23S
Drk661			7200S		09H 53M 45S
Drk662			7200S		11H 54M 07S
Drk663	-----		7200S		13H 54M 29S
PHD664		70000FRs			16H 44M 13S
Drk665			7200S		18H 01M 03S
					1999/10/11
DEP666				29100S	10H 22M 33S
Drk667			7200S		15H 57M 58S
DEP668				54000S	17H 58M 22S
					1999/10/12
Bin669			7200S		08H 58M 46S
Drk670			7200S		10H 59M 03S
\\/\	Fuel Test	1min	Day-5	13:09 - 13:10	1999/10/12
\\/\					
Drk671			0300S		13H 10M 36S
Drk672			0300S		13H 16M 00S
Drk673			0300S		13H 21M 23S
Drk674			0300S		13H 26M 46S
Drk675			0300S		13H 32M 09S
Pin676	L=1 1800S				14H 22M 34S
Pin677	L=5 1800S				14H 57M 10S
\\/\					
	15 hour	Day-6	16:00 - 07:00		1999/10/12
\\/\					
					1999/10/13
Drk678			0300S		07H 02M 18S
Drk679			0300S		07H 07M 41S
Drk680			0300S		07H 13M 04S
Drk681			0300S		07H 18M 27S
Drk682			0300S		07H 23M 50S
Drk683			7200S		07H 29M 14S
Drk684			7200S		09H 29M 37S
PHD685		70000FRs			11H 31M 49S
Drk686			7200S		13H 05M 54S
Drk687			7200S		15H 06M 17S
Drk688			7200S		17H 06M 40S
Drk689			7200S		19H 07M 03S
Drk690			7200S		21H 07M 26S
Drk691			7200S		23H 07M 49S

[illegible]

[illegible]

[illegible]

File Name	Pinhole	PHD	Dark	F-F	Time(start)
Drk860			7200S		20H 38M 02S
Drk861			7200S		22H 38M 28S
					1999/11/07
Drk862			7200S		00H 38M 54S
Drk863			7200S		02H 39M 20S
					1999/11/08
PHD864		70000FRs			11H 17M 17S
Ana865		(256V)	Blue	30000FRs	12H 17M 42S
					1999/11/09
DEP866		TH=8	Blue	54000S	10H 12M 37S
					1999/11/10
Drk867			7200S		01H 13M 13S
Drk868			7200S		03H 13M 46S
Drk869			7200S		05H 14M 19S
Drk870			7200S		07H 14M 52S
Drk871			7200S		09H 15M 25S
PHD872		70000FRs			15H 00M 10S
DEP873		TH=8	Blue	54000S	17H 51M 10S
					1999/11/11
Drk874			7200S		08H 51M 40S
Drk875			7200S		10H 54M 00S
Drk876			7200S		12H 54M 35S
Drk877			7200S		14H 55M 10S
Drk878			7200S		16H 55M 45S
DEP879		TH=8	Red	54000S	20H 00M 25S
					1999/11/12
Drk880			7200S		11H 01M 01S
Ana881		(256V)	Red	30000FRs	13H 11M 26S
PHD882		70000FRs			17H 42M 34S

Effect of Fluorescence on F-F at Peak

Total dose (hour)	Pinhole intensity (counts/sec)									
	120c/s	210	1.1k	2.1k	19k	21k	220k	320k	2070k	2070k
Blue										
0.3 hr	.000	.000	.000	.000	.000	.000	.011	.011	.038	.036
1.0 hr	.000	.000	.000	.000	.000	.000	.001	.002	.005	.006
3.0 hr	.000	.000	.000	.000	.000	.000	.002	.003	.005	.006
7.0 hr	.000	.000	.000	.000	.002	.002	.006	.006	.010	.011
15.0 hr	.000	.000	.000	.000	.000	.002	.005	.006	.006	.007
30.0 hr	.000	.000	.000	.000	.003	.002	.007	.008	.007	.005
50.0 hr	.000	.000	.000	.000	.001	.002	.003	.003	.001	.002
70.0 hr	.000	.000	.001	.000	.003	.003	.005	.004	.001	.001
100.0 hr	.000	.000	.000	.001	.003	.003	.006	.005	-.001	-.000
100.0 hr	.000	.000	.001	.000	.002	.002	.004	.003	-.001	-.000
100.0 hr	.000	.000	.000	.000	.001	.001	.001	.001	.000	.000
Green										
100.0 hr	.000	.000	-.000	.000	.001	.000	.001	.001	.000	.000
Red										
100.0 hr	.000	.000	.000	.000	.001	.001	.000	.000	.000	.000
Threshold level = 8ADU										
Blue										
100.0 hr	.000	.000	.000	.000	.001	.000	-.001	.000	.000	.000
100.0 hr	.000	.000	.000	.000	.000	-.000	-.000	-.000	.000	.000
100.0 hr	.000	.000	-.000	.000	.000	.001	-.001	.000	.000	.000
Green										
100.0 hr	.000	.000	-.000	.000	.000	.001	.000	-.000	.000	.000
Red										
100.0 hr	.000	.000	.000	.000	-.000	.001	.001	.000	.000	.000
100.0 hr	.000	.000	.000	.000	.001	.001	-.000	-.000	.000	.000
100.0 hr	.000	.000	-.000	-.000	-.000	.001	-.001	-.001	.000	.000

Effect of Fluorescence on F-F (Average over circle D=213um)

Total dose		Pinhole intensity (counts/sec)								
(hour)	120c/s	210	1.1k	2.1k	19k	21k	220k	320k	2070k	2070k
Blue										
0.3 hr	.000	.000	.000	.000	.000	.000	.007	.008	.027	.025
1.0 hr	.000	.000	.000	.000	.001	.000	.001	.001	.004	.004
3.0 hr	.000	.000	.000	.000	.000	.000	.002	.002	.004	.004
7.0 hr	.000	.000	.000	.000	.001	.001	.005	.004	.009	.009
15.0 hr	.000	.000	.000	.000	.001	.002	.004	.004	.007	.008
30.0 hr	.000	.000	.000	.000	.002	.002	.006	.007	.008	.007
50.0 hr	.000	.000	.000	.000	.001	.001	.003	.002	.002	.002
70.0 hr	.000	.000	.001	.001	.003	.002	.004	.004	.003	.003
100.0 hr	.000	.000	.001	.001	.003	.003	.005	.005	.003	.003
100.0 hr	.000	.000	.001	.001	.002	.002	.004	.003	.001	.002
100.0 hr	.000	.000	.000	.000	.001	.001	.001	.001	.000	.000
Green										
100.0 hr	.000	.000	-.000	.000	.001	.000	.001	.001	.000	.000
Red										
100.0 hr	.000	.000	.000	.001	.001	.001	.000	.000	-.000	-.000
Threshold level = 8ADU										
Blue										
100.0 hr	.000	.000	.000	.001	.001	.000	-.001	.000	-.001	-.000
100.0 hr	.000	.000	.000	.001	.000	-.000	-.000	-.000	-.001	-.001
100.0 hr	.000	.000	-.000	.000	.000	.001	-.001	.000	-.001	-.000
Green										
100.0 hr	.000	.000	-.000	.000	.000	.001	.000	-.000	-.001	-.001
Red										
100.0 hr	.000	.000	.000	.001	-.000	.000	.001	.000	-.001	-.000
100.0 hr	.000	.000	-.000	.001	.001	.000	-.000	-.000	-.001	-.001
100.0 hr	.000	.000	-.000	-.000	-.000	.001	-.001	-.001	-.001	-.001

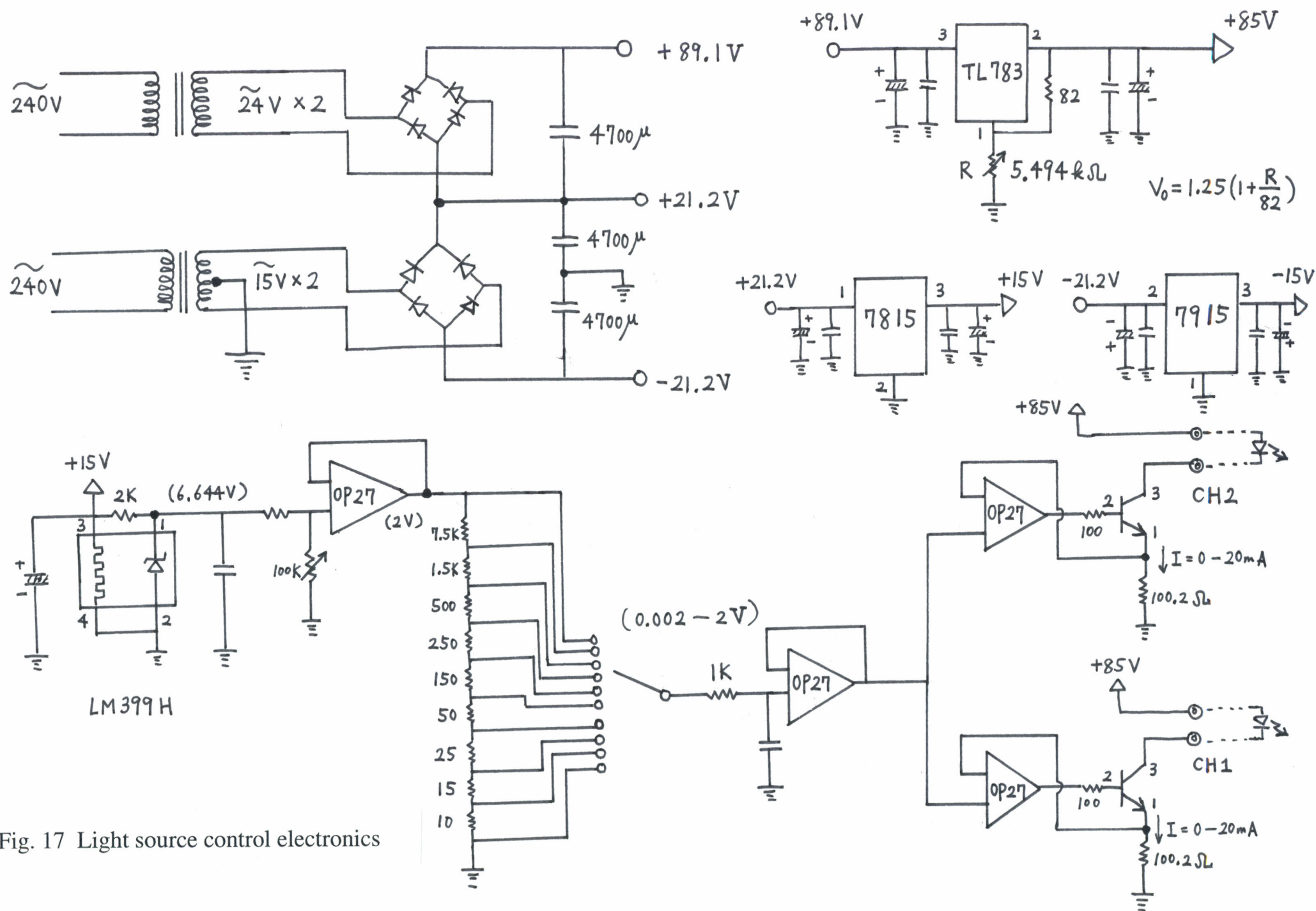


Fig. 17 Light source control electronics

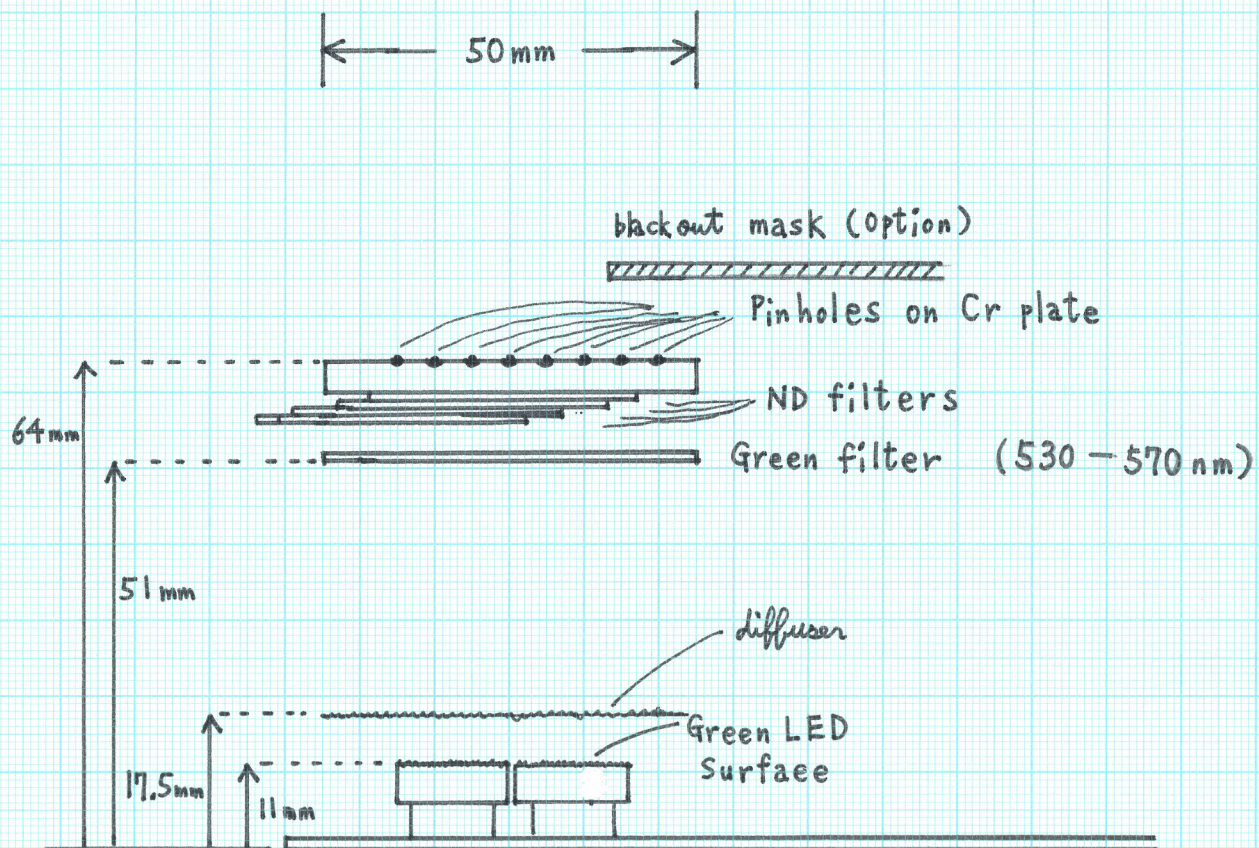
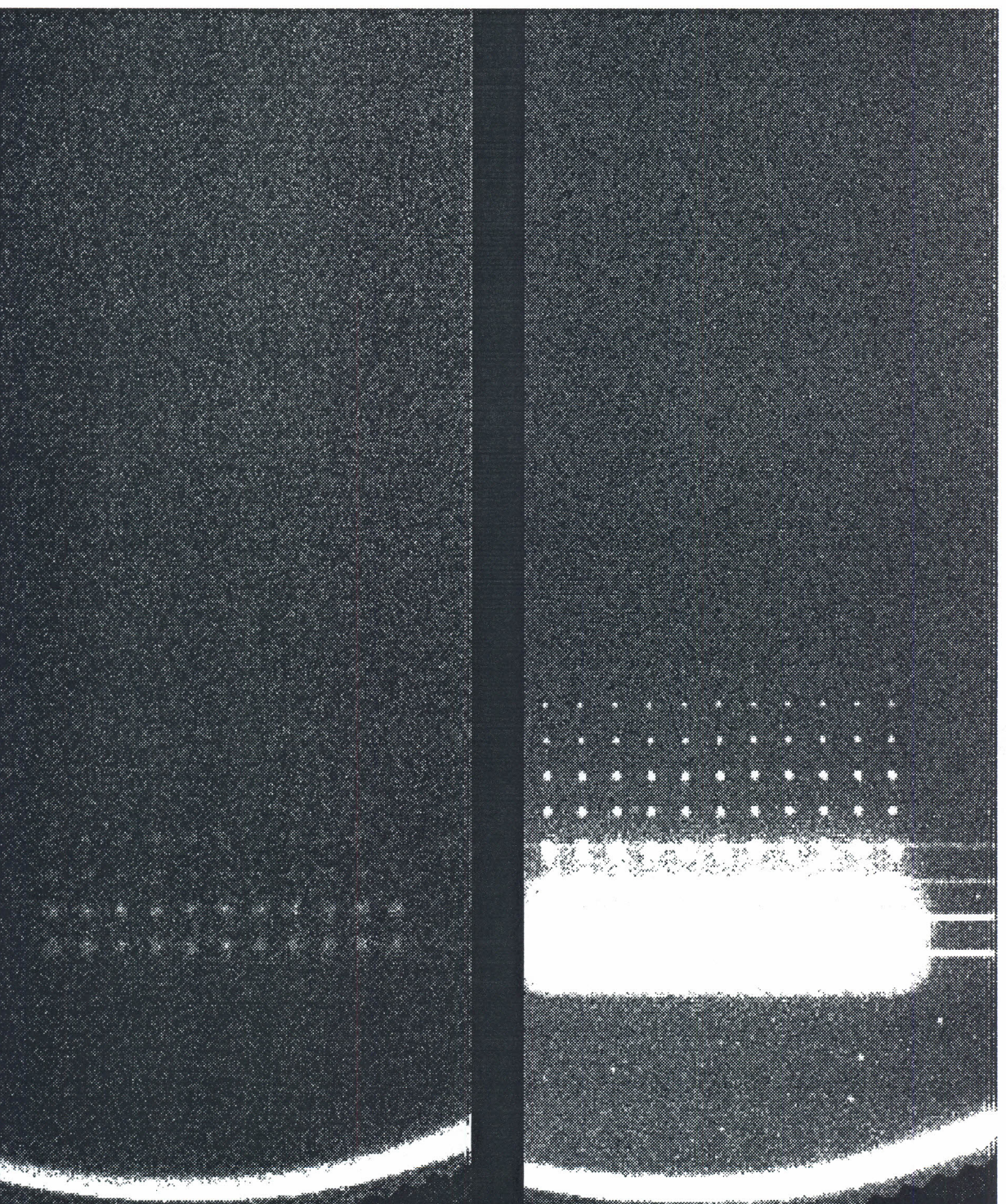


Fig. 18 Pinhole light source

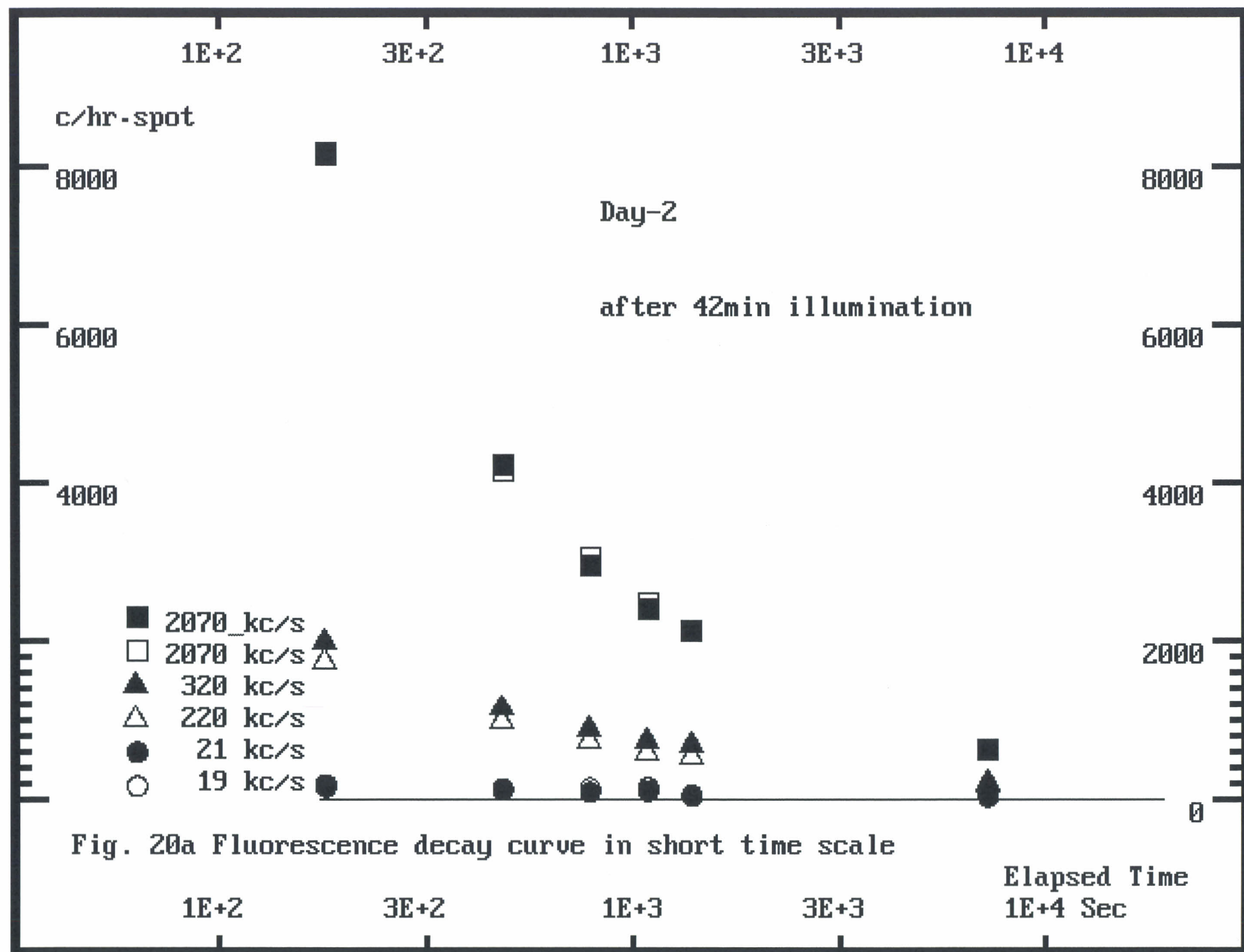


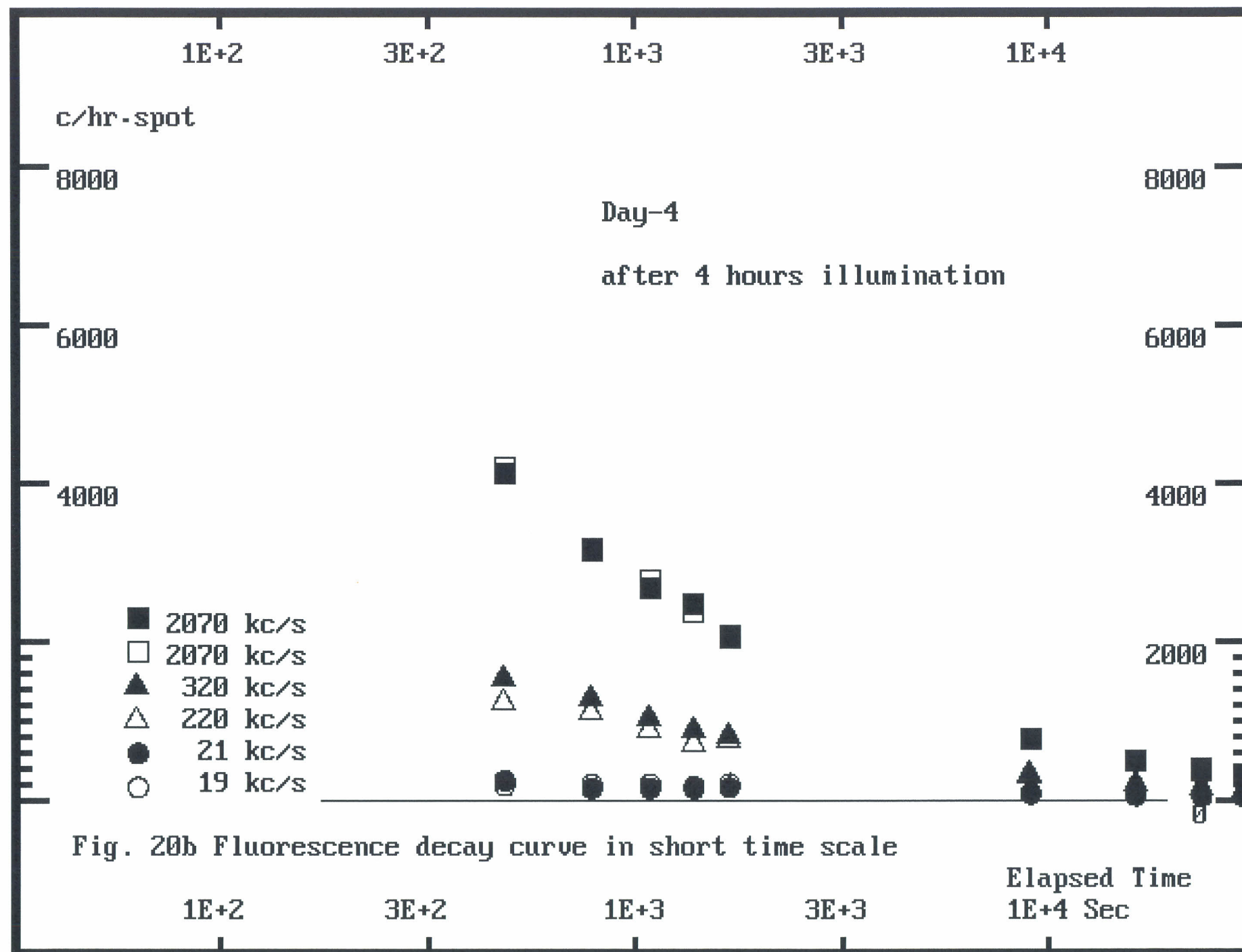
11x11 array of
pinhole

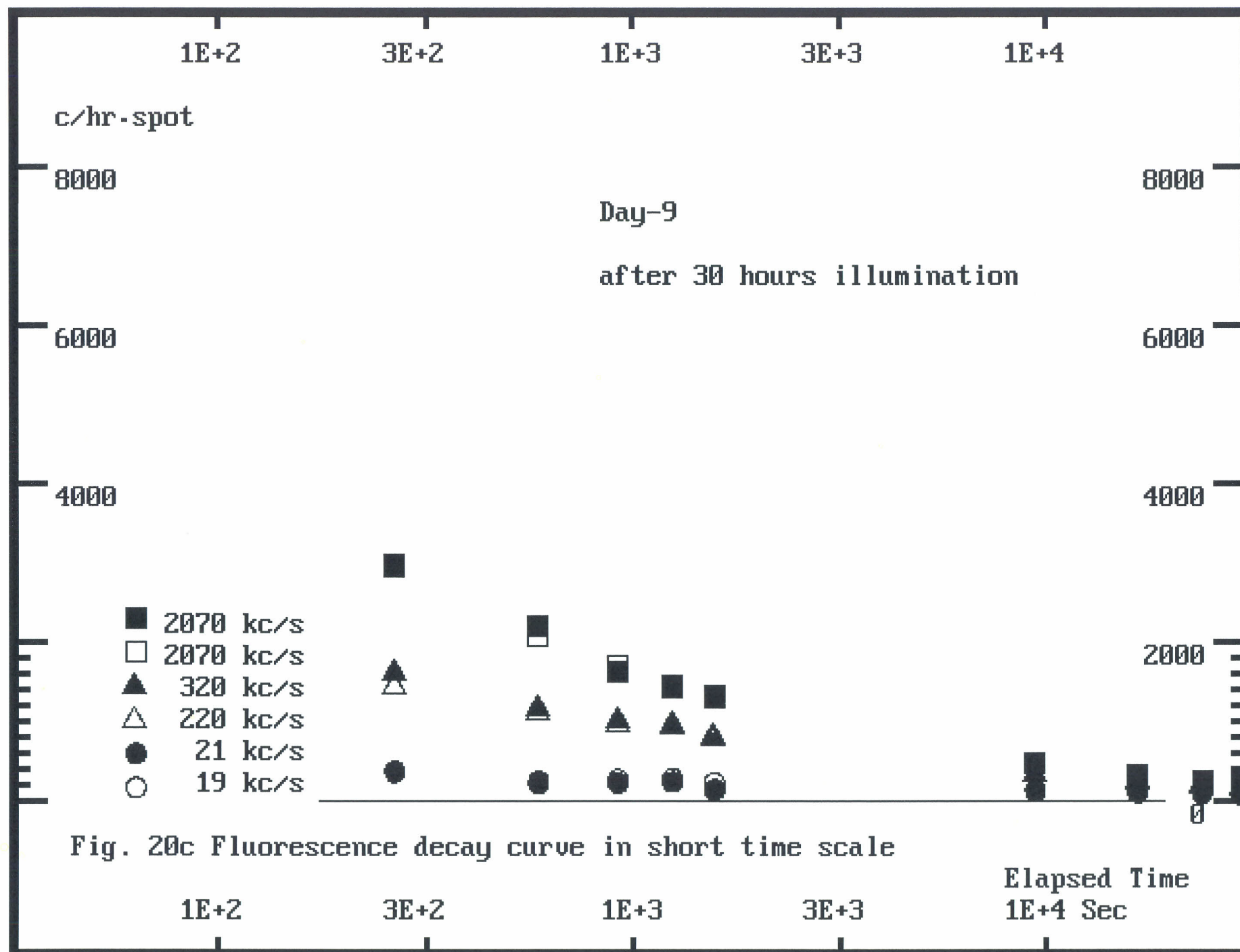
Fluorescence
100min after
10 min illumi-
nation.

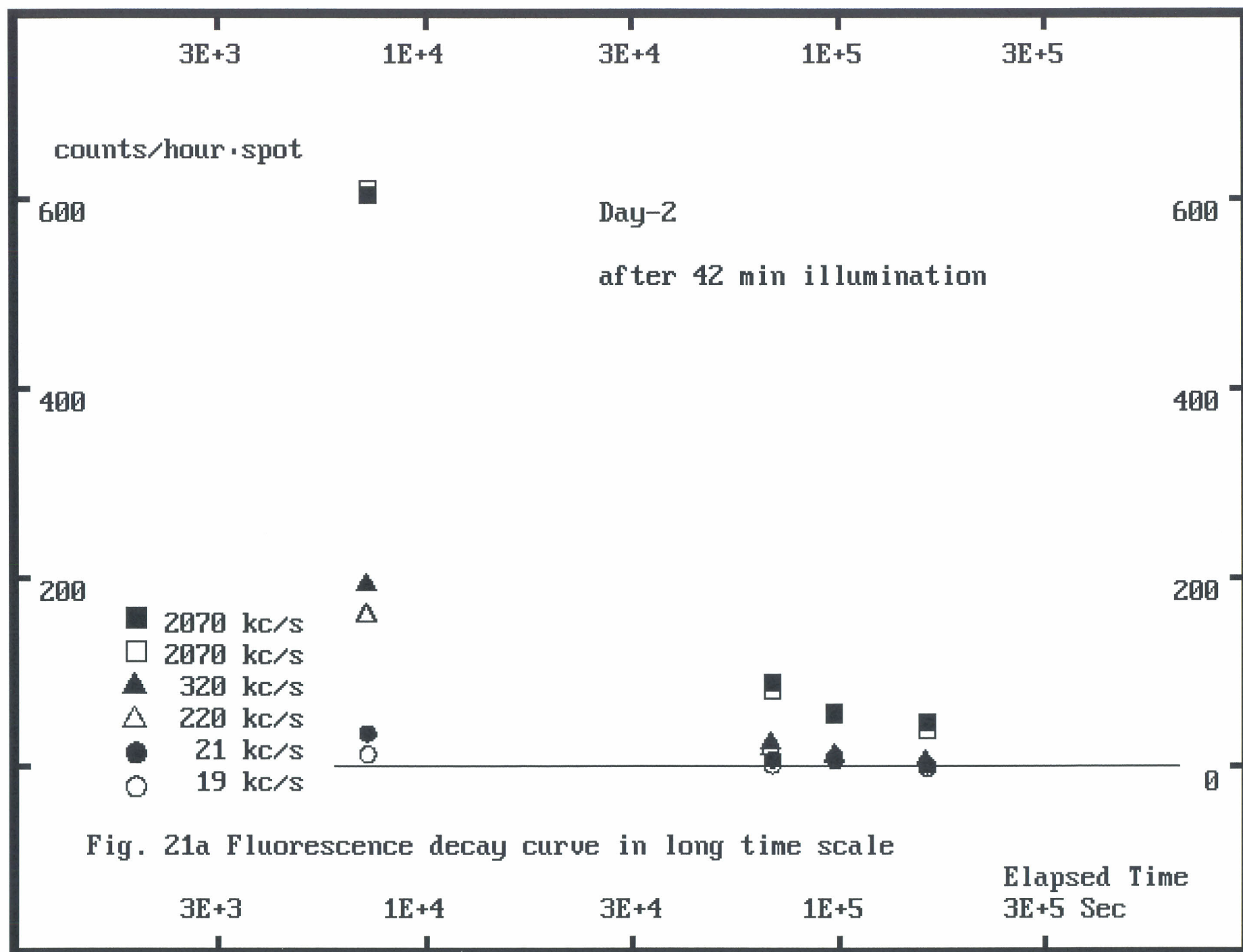
Day-1

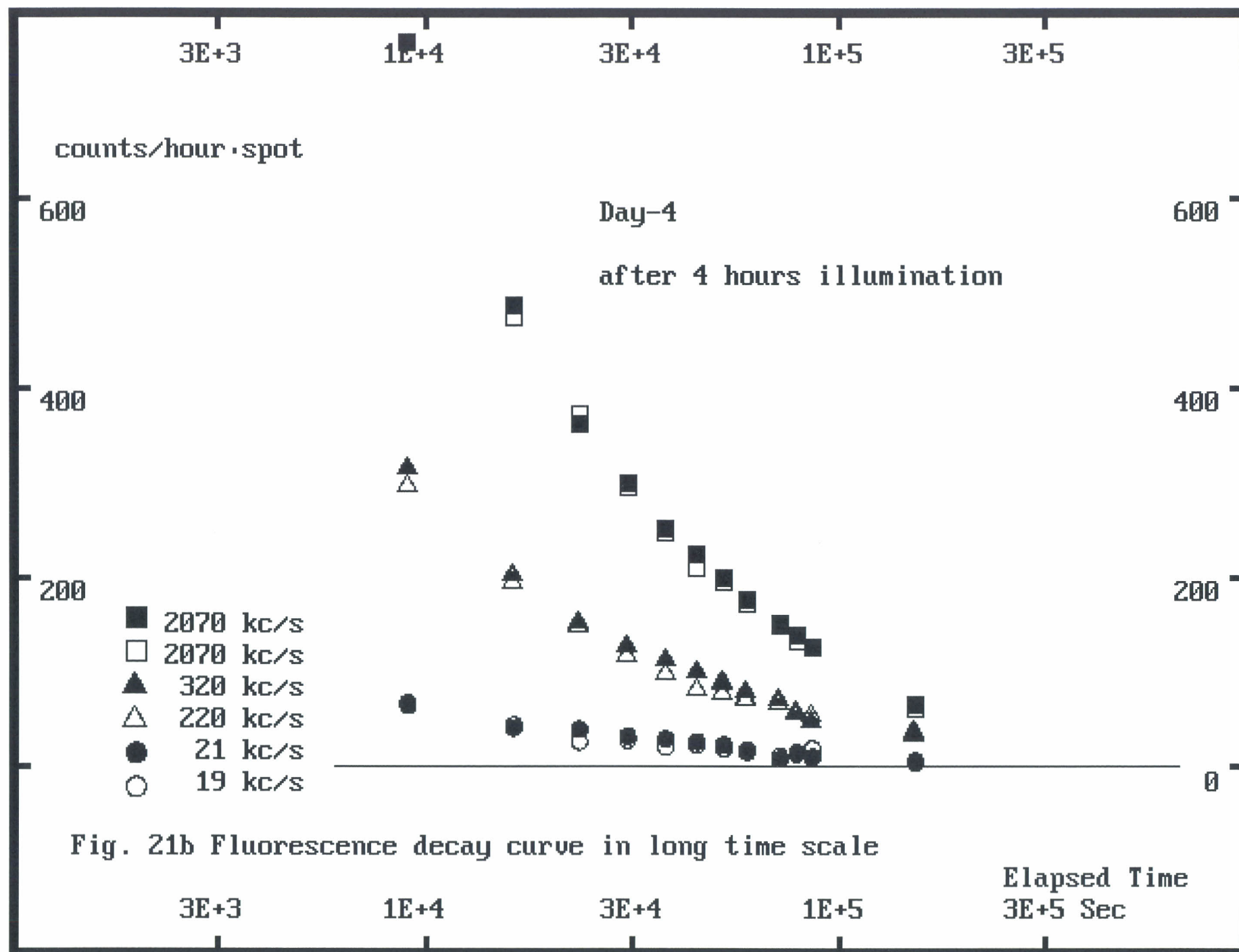
Fig. 19 Intense illumination by pinhole array and fluorescence DEP_#8 tube

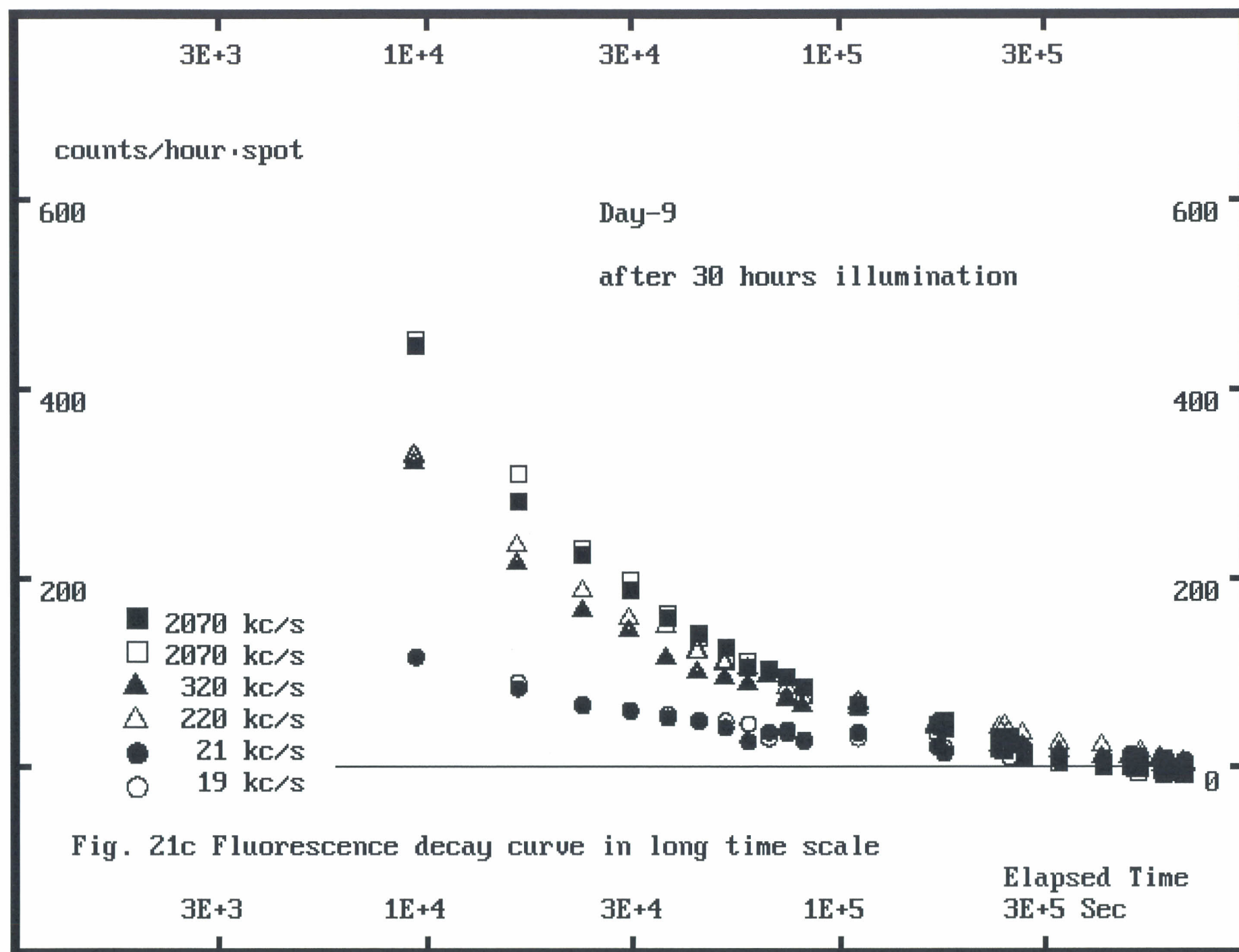












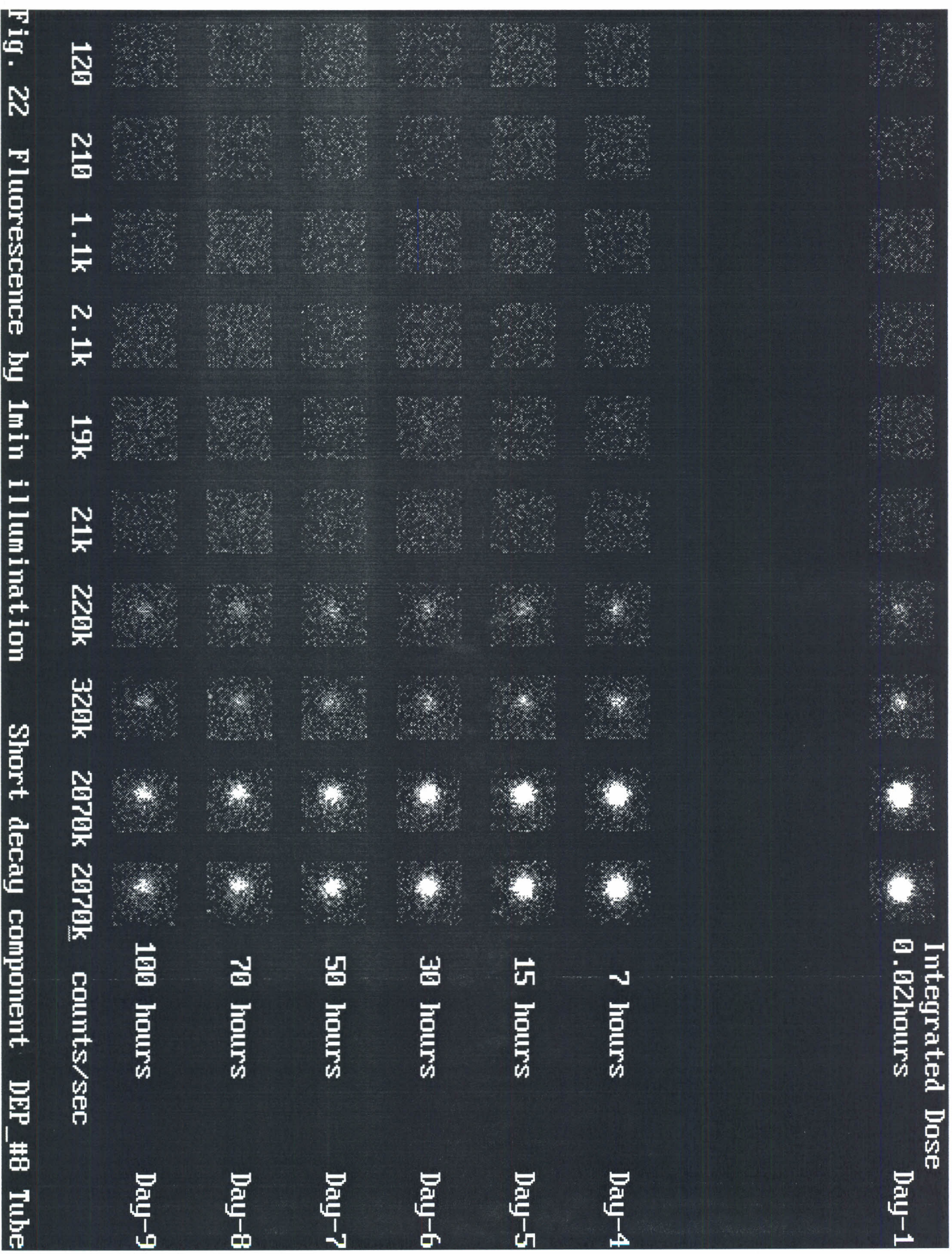


Fig. 22 Fluorescence by 1min illumination Short decay component DEP_#8 Tube

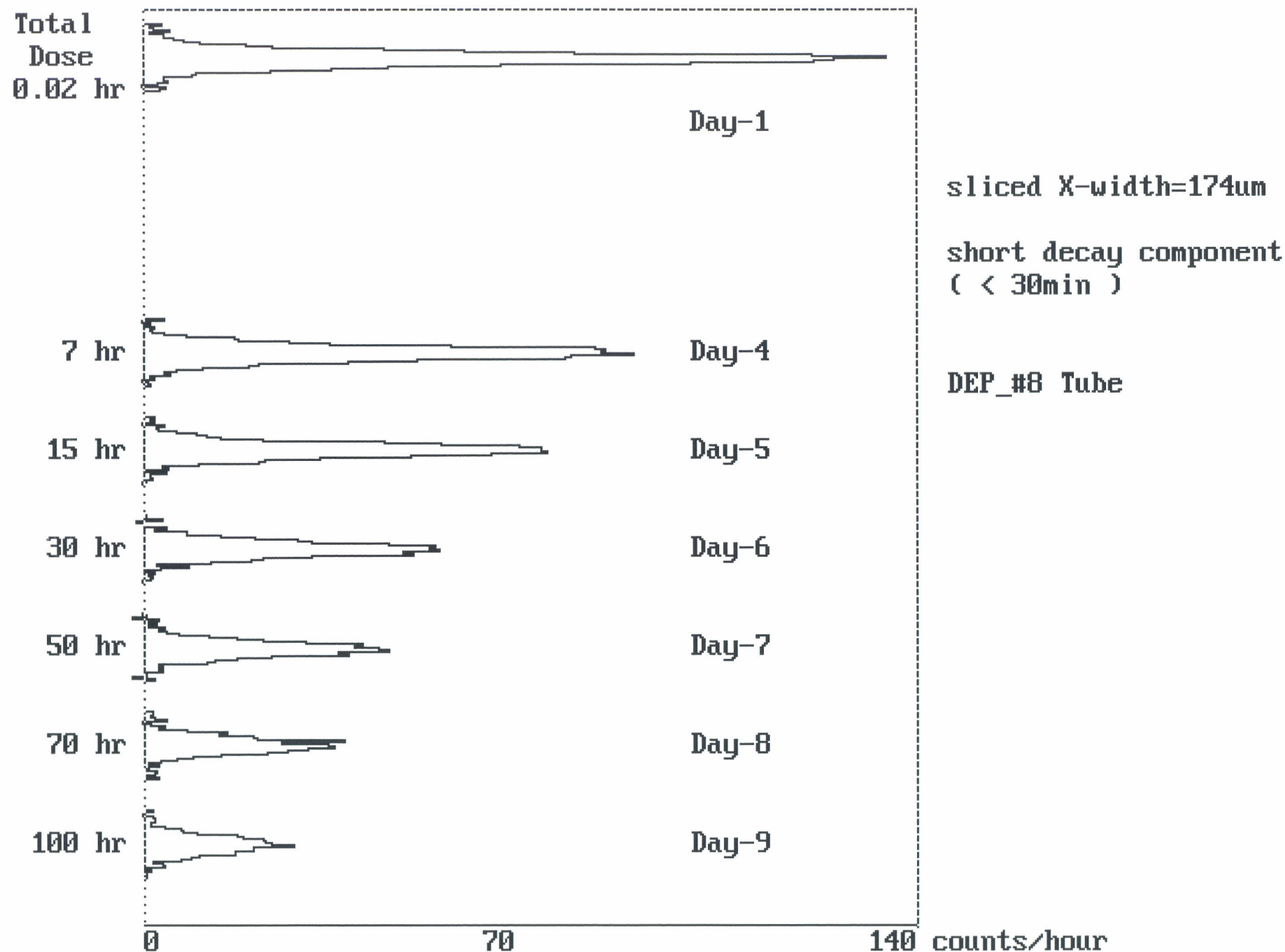
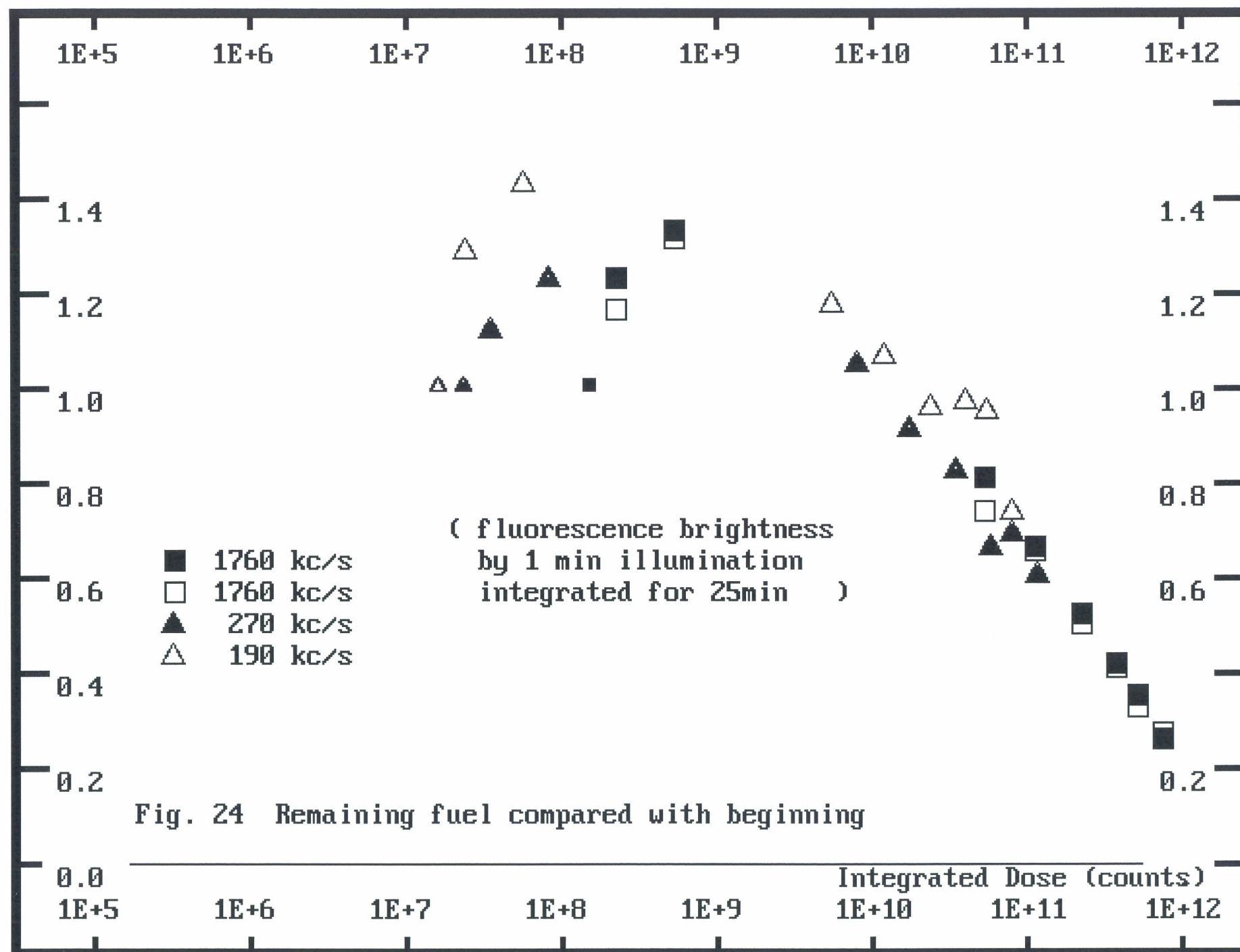


Fig. 23 Fluorescence after 1 min illumination by $2E+6$ c/s pinholes



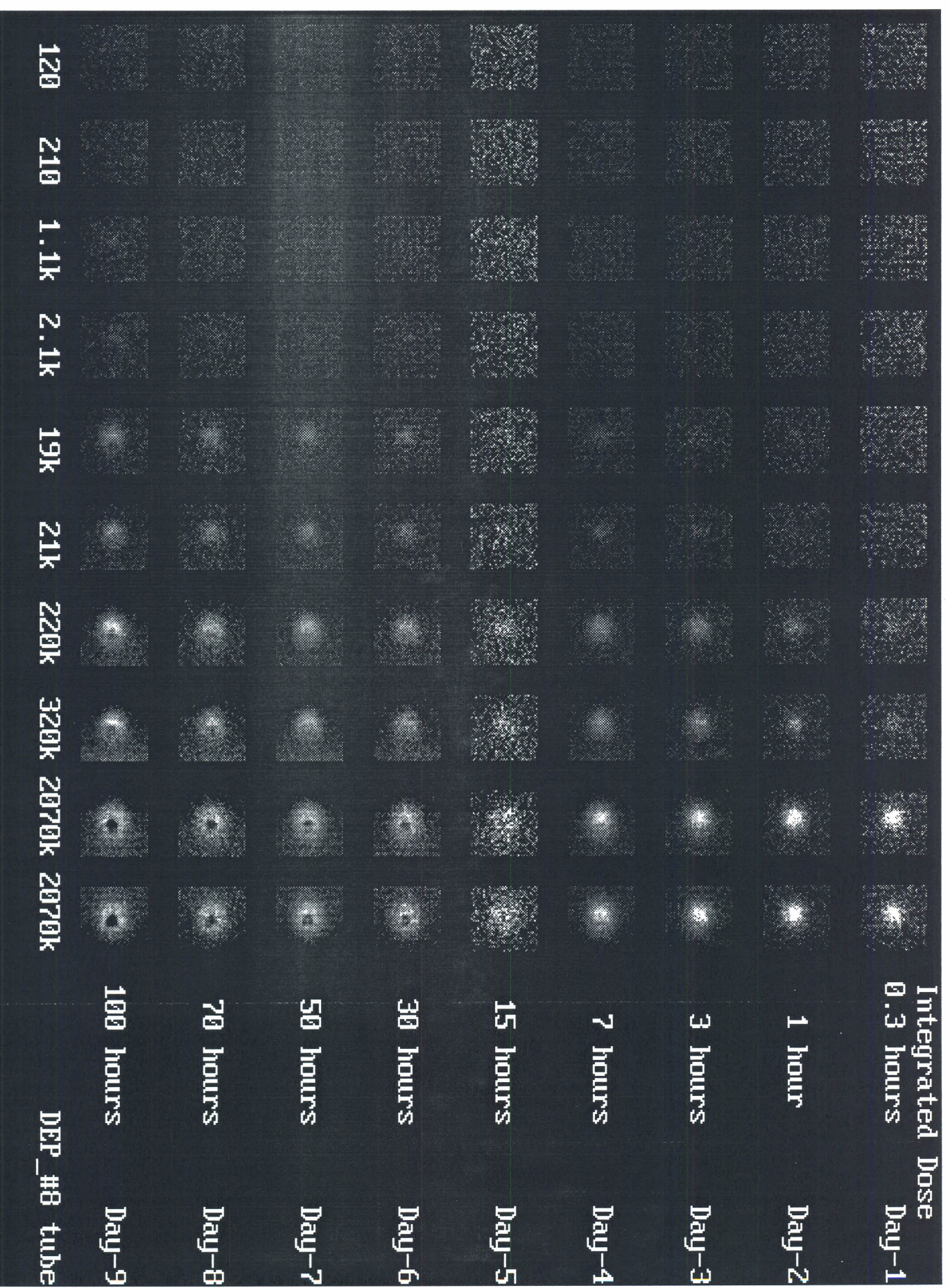


Fig. 25 Day by day change of fluorescence Long decay component

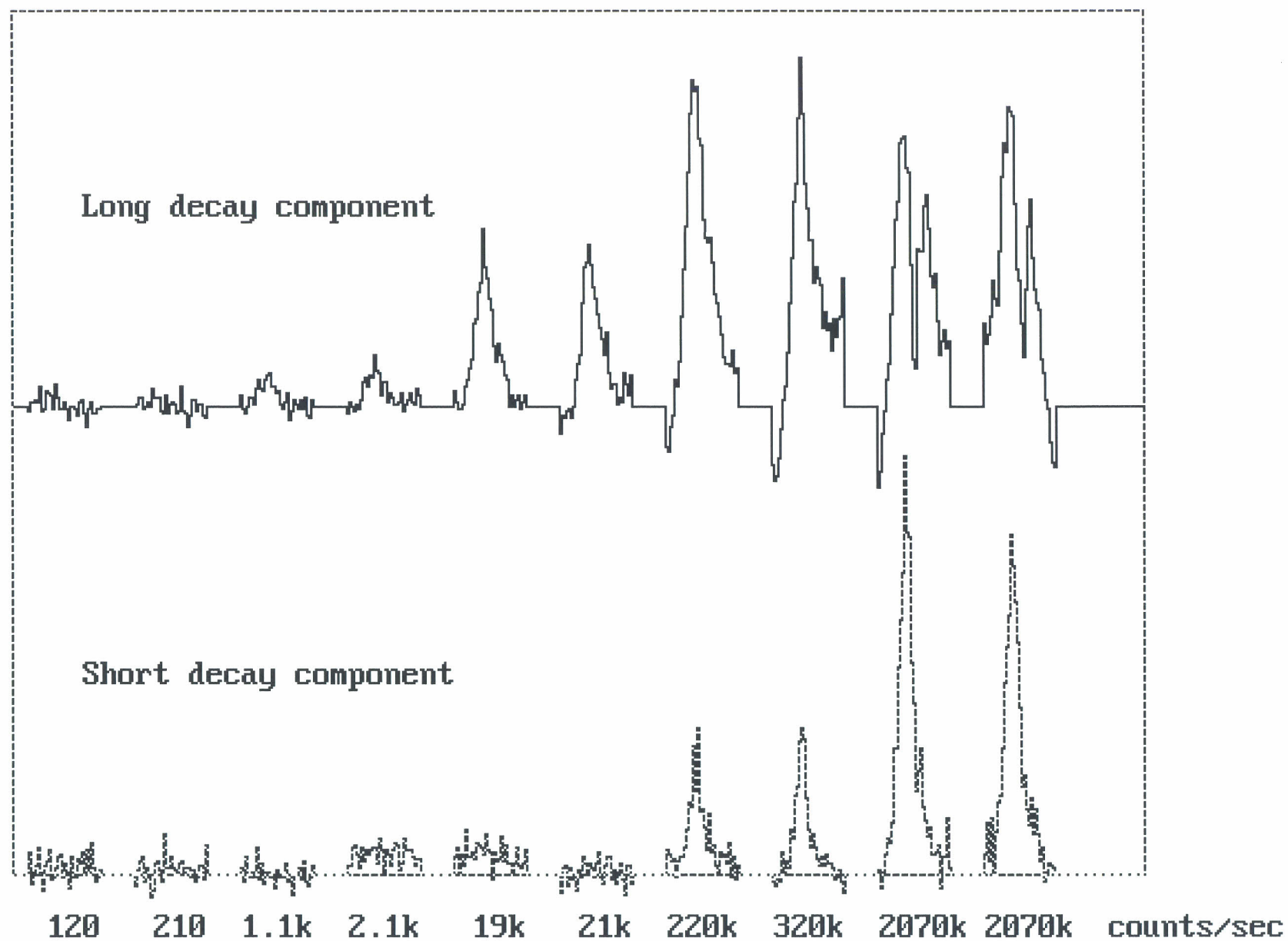


Fig. 26 Profiles of fluorescence after 100 hours dose

DEP_#8 Tube

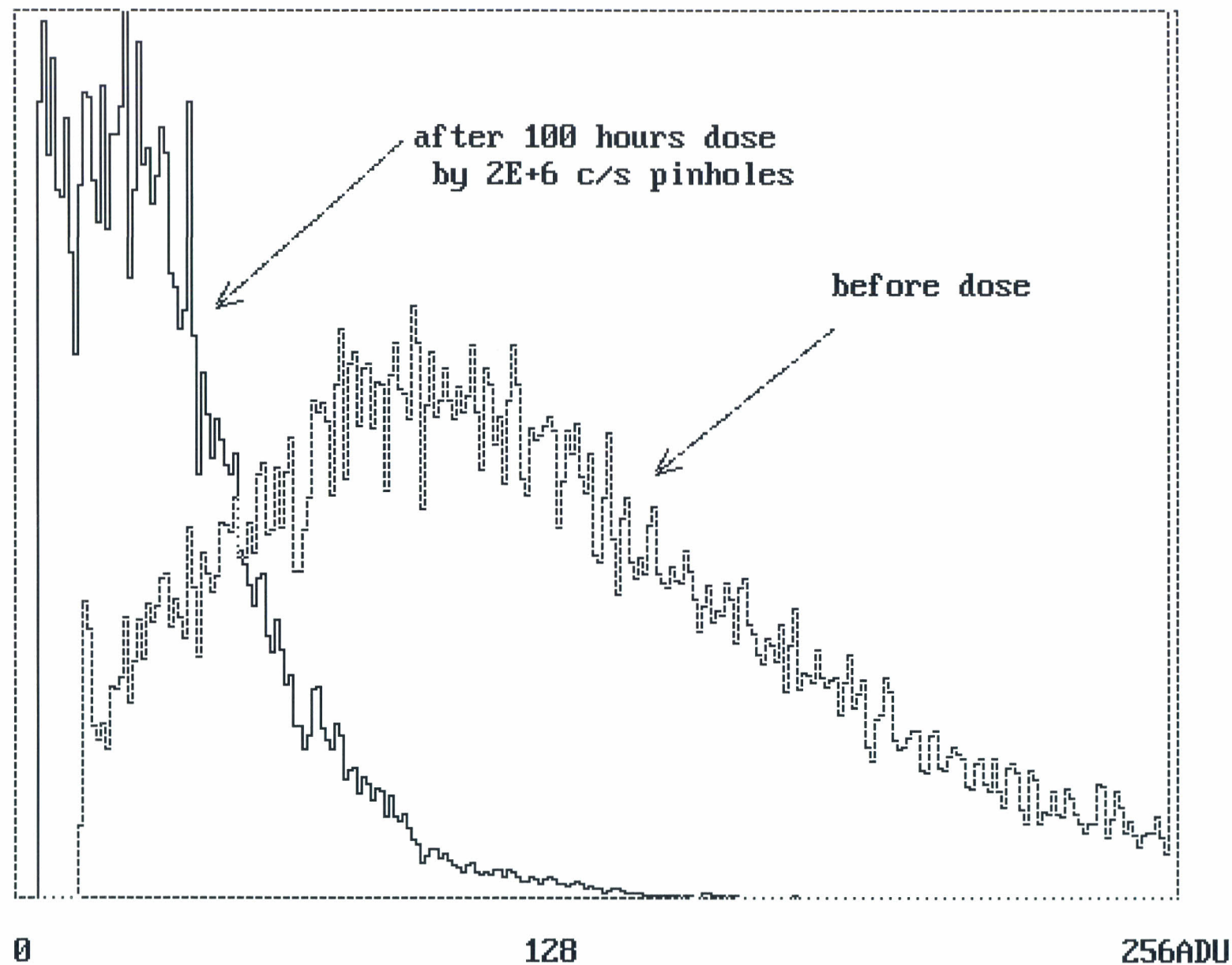


Fig. 27a Pulse height distributions before and after 100 hours dose

DEP_#8

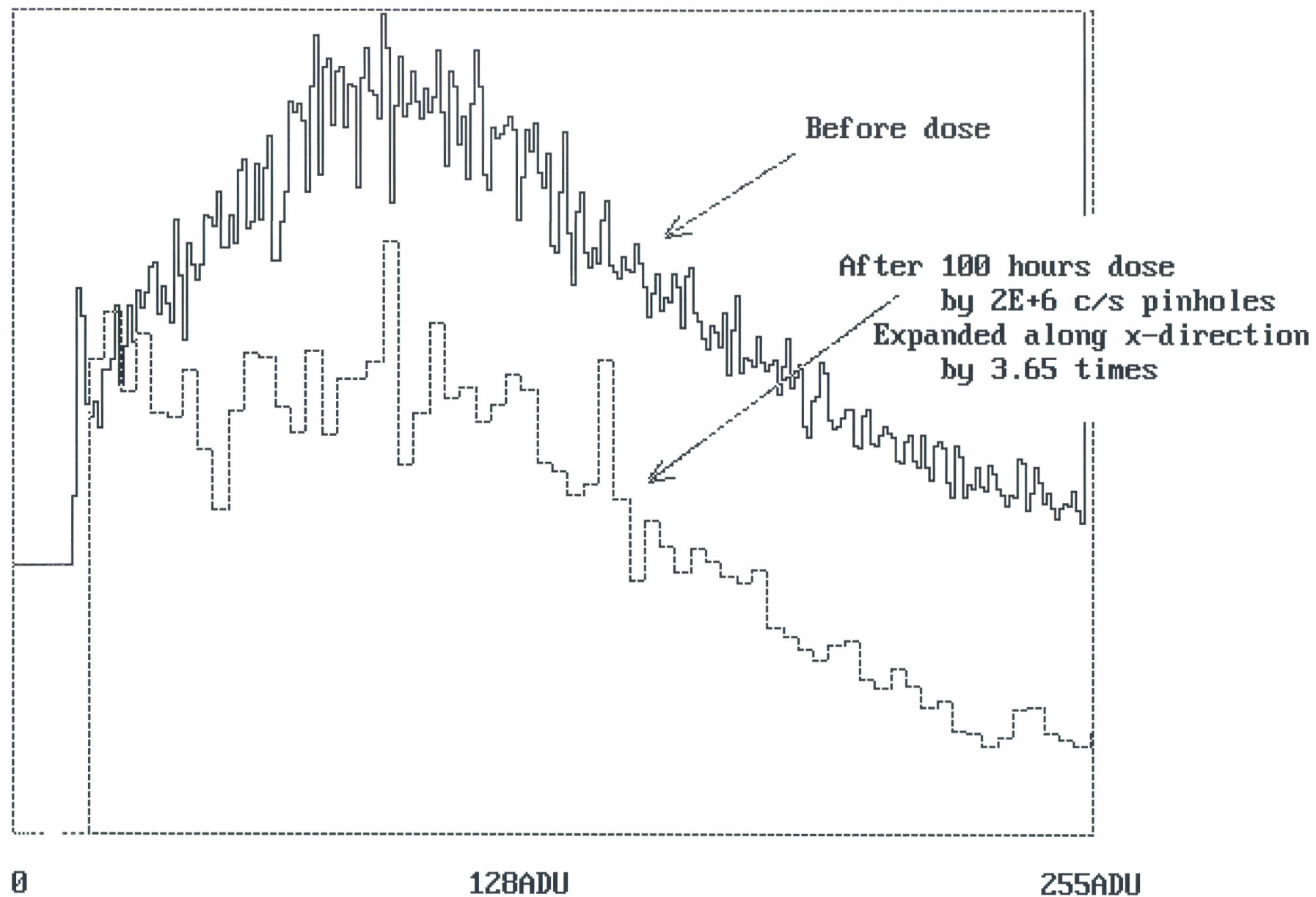
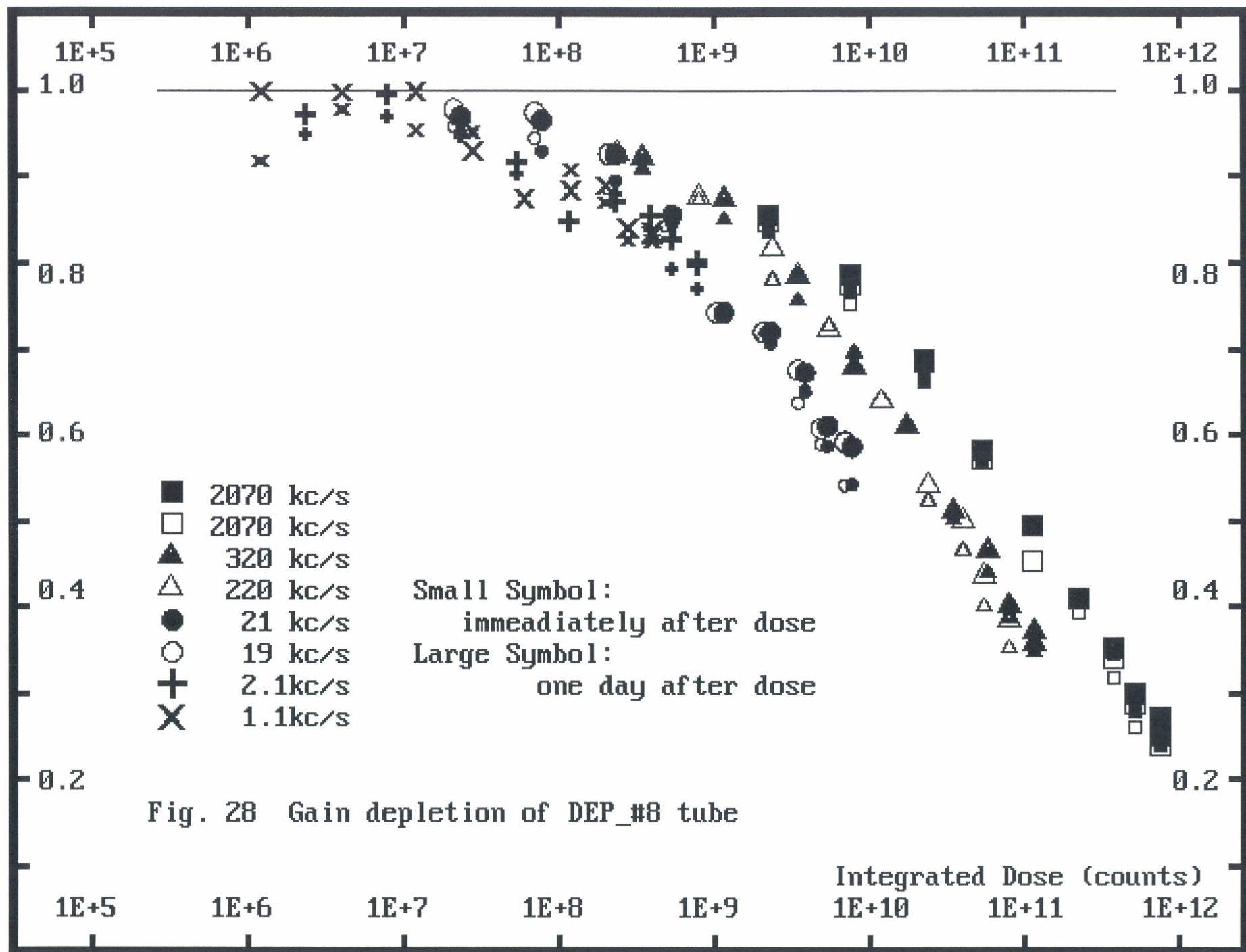
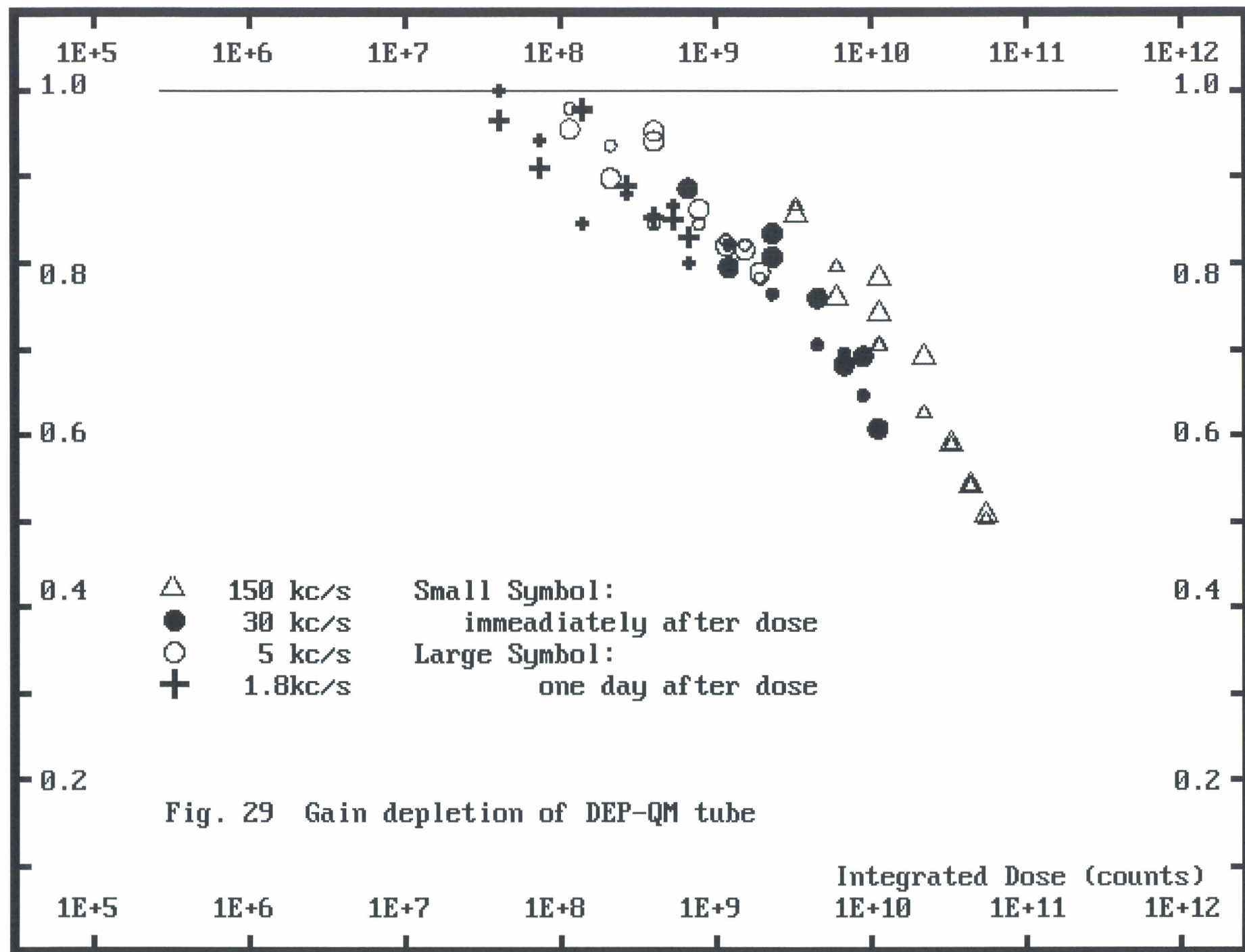
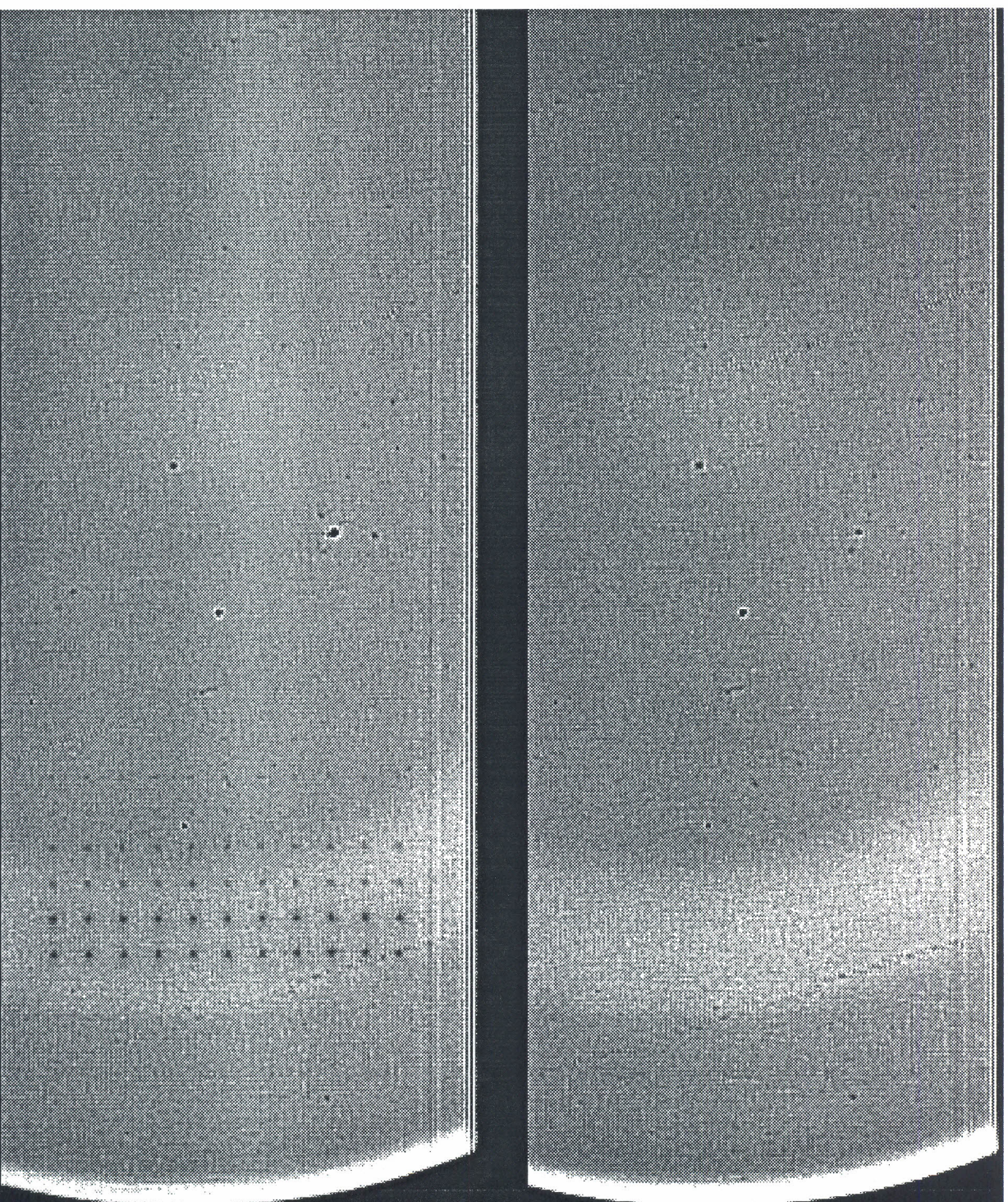


Fig. 27b Pulse height distributions before and after 100 hours dose DEP_#8





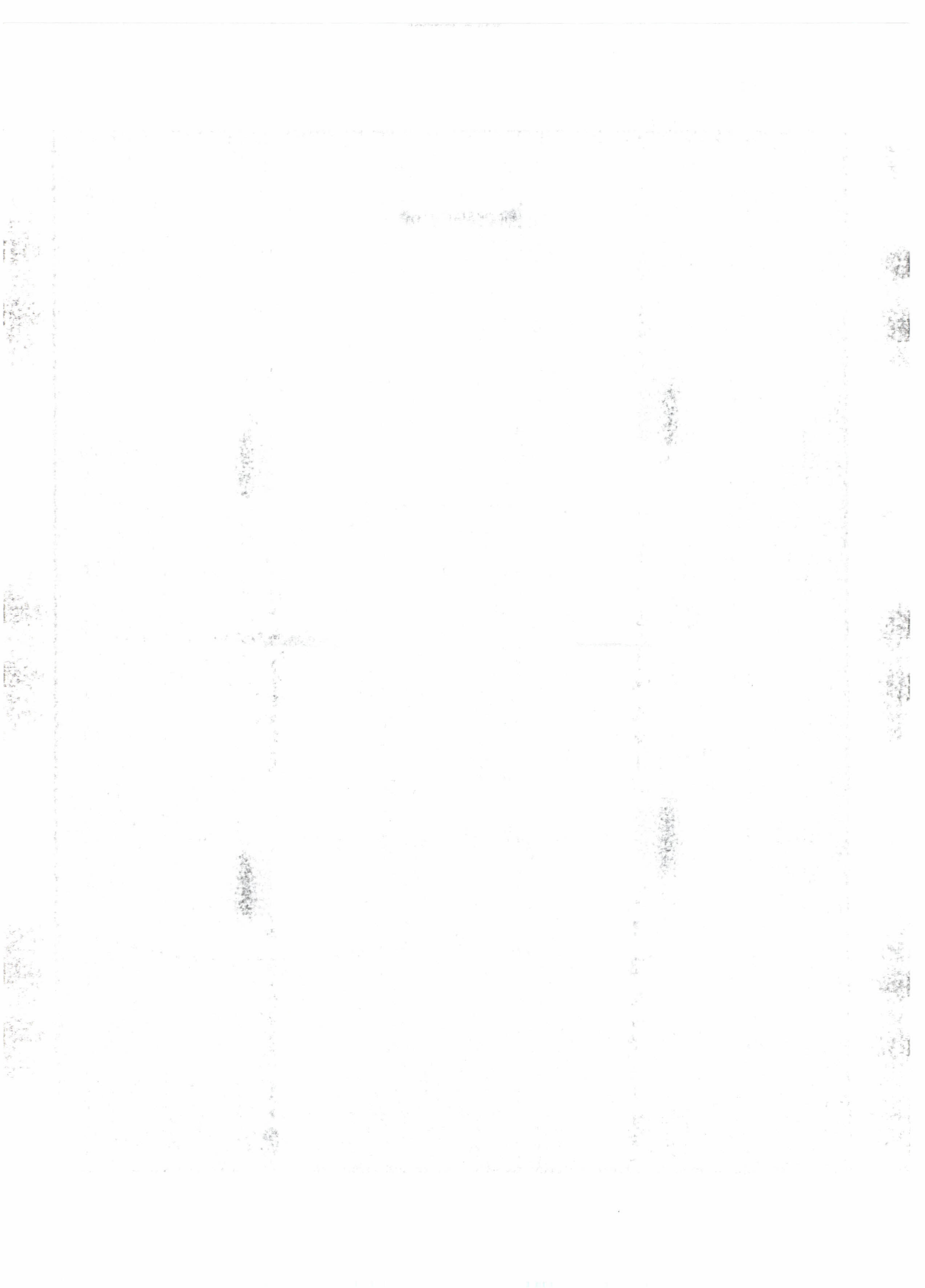


Before dose

After 100 hours
illumination

Blue LED, DEP_#8 tube

Fig. 30 F-F images acquired in photon counting mode, before and after Dose



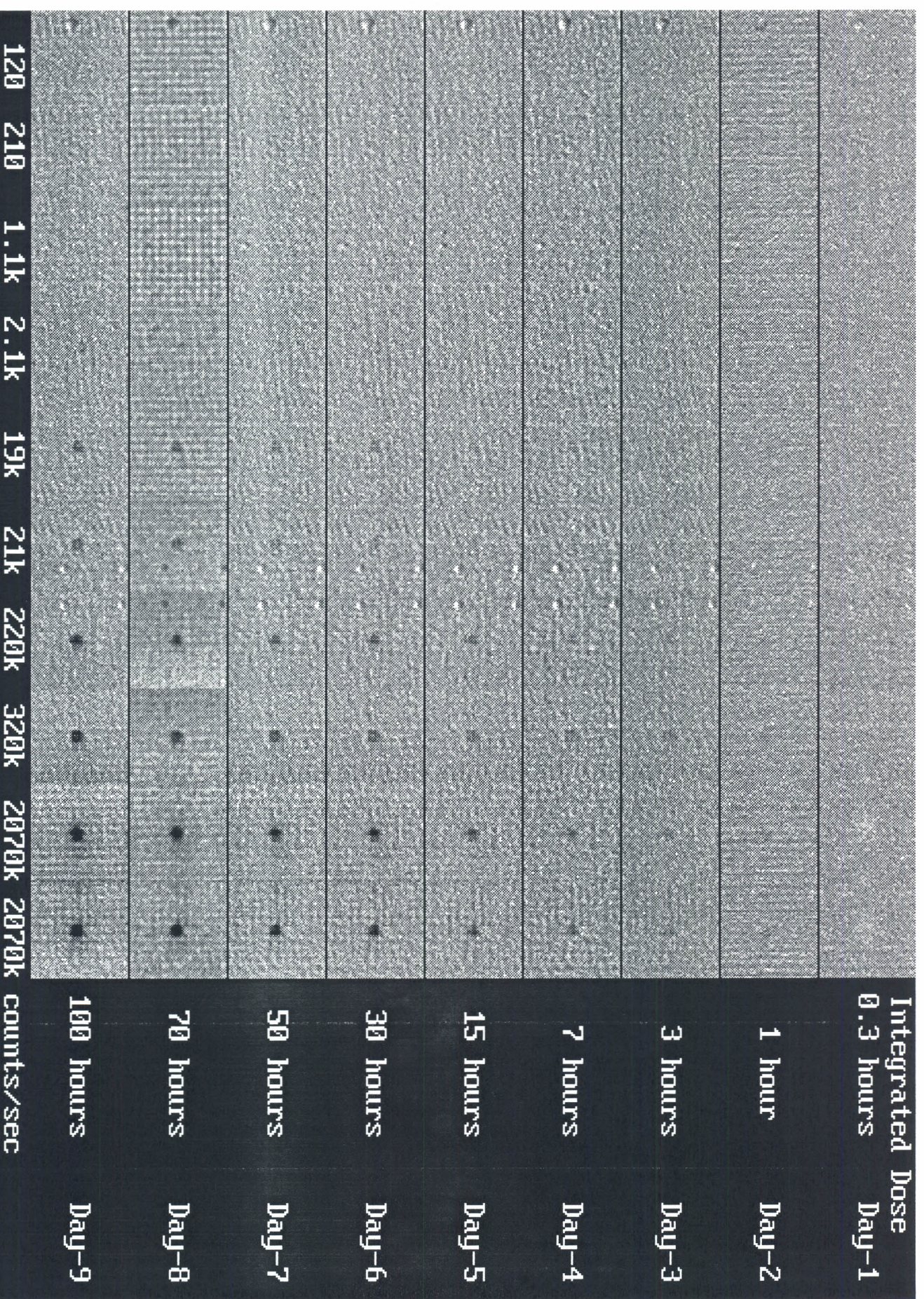


Fig. 31 Day by day change of black spots in F-F 11 spots are averaged DEF_#8

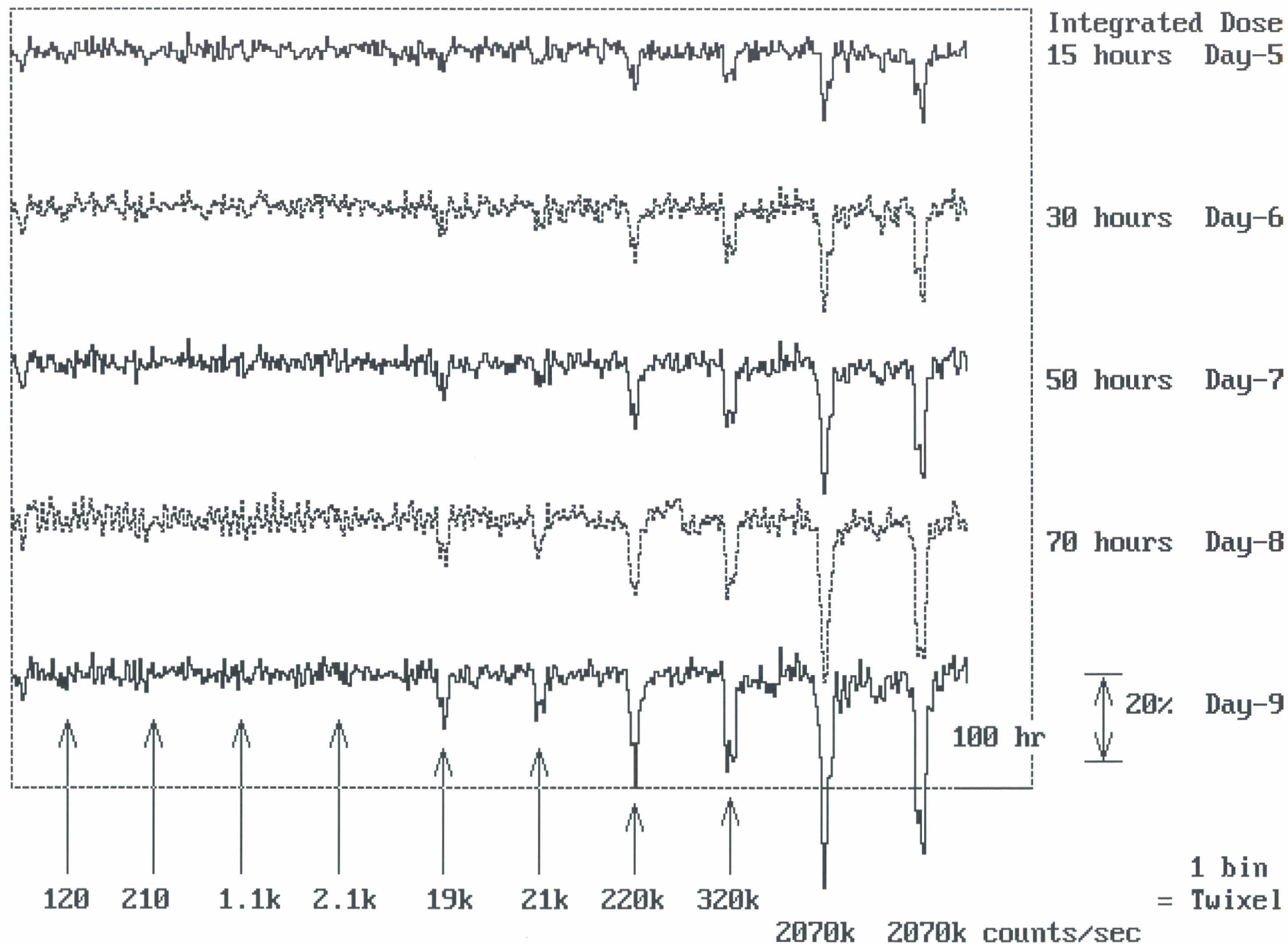
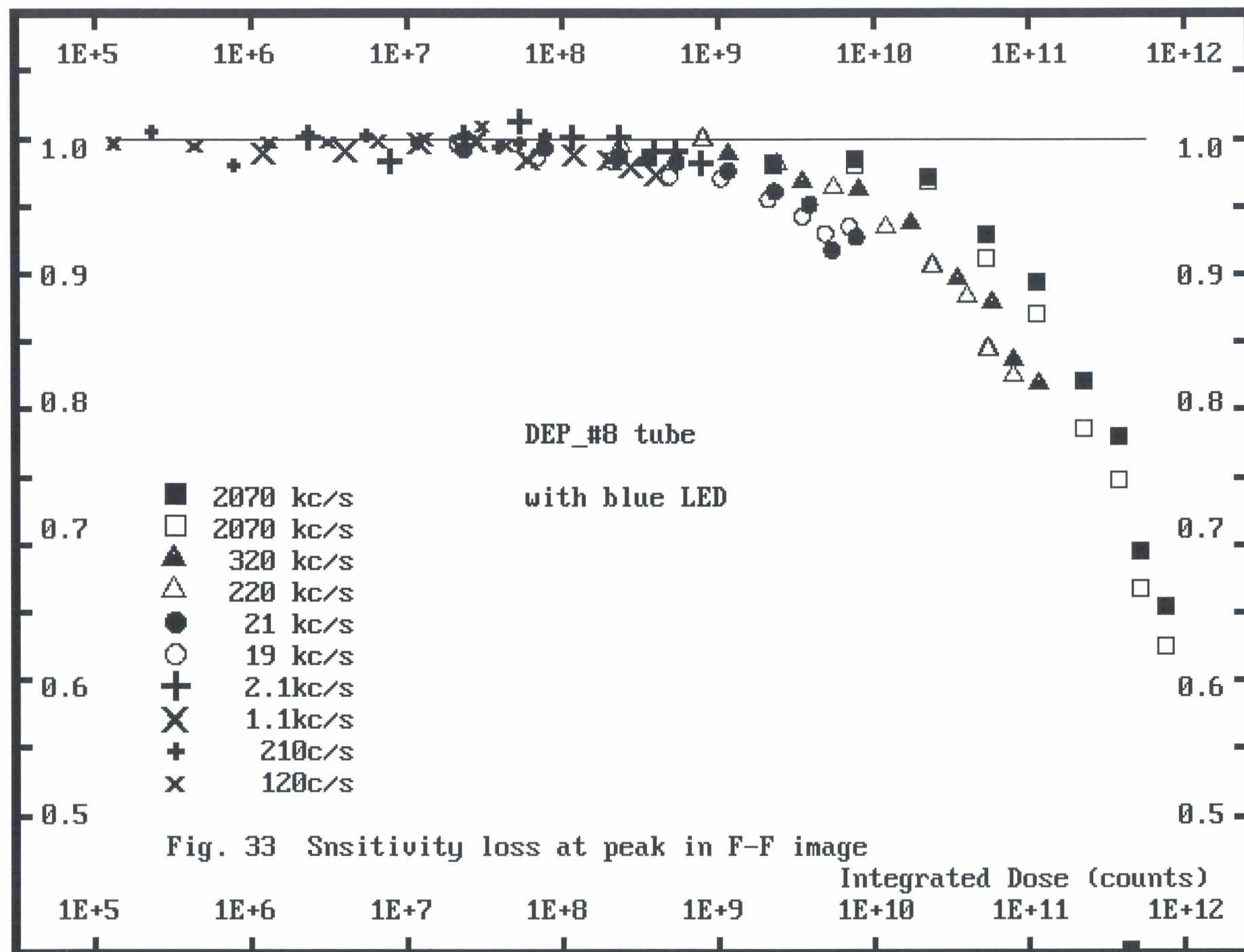
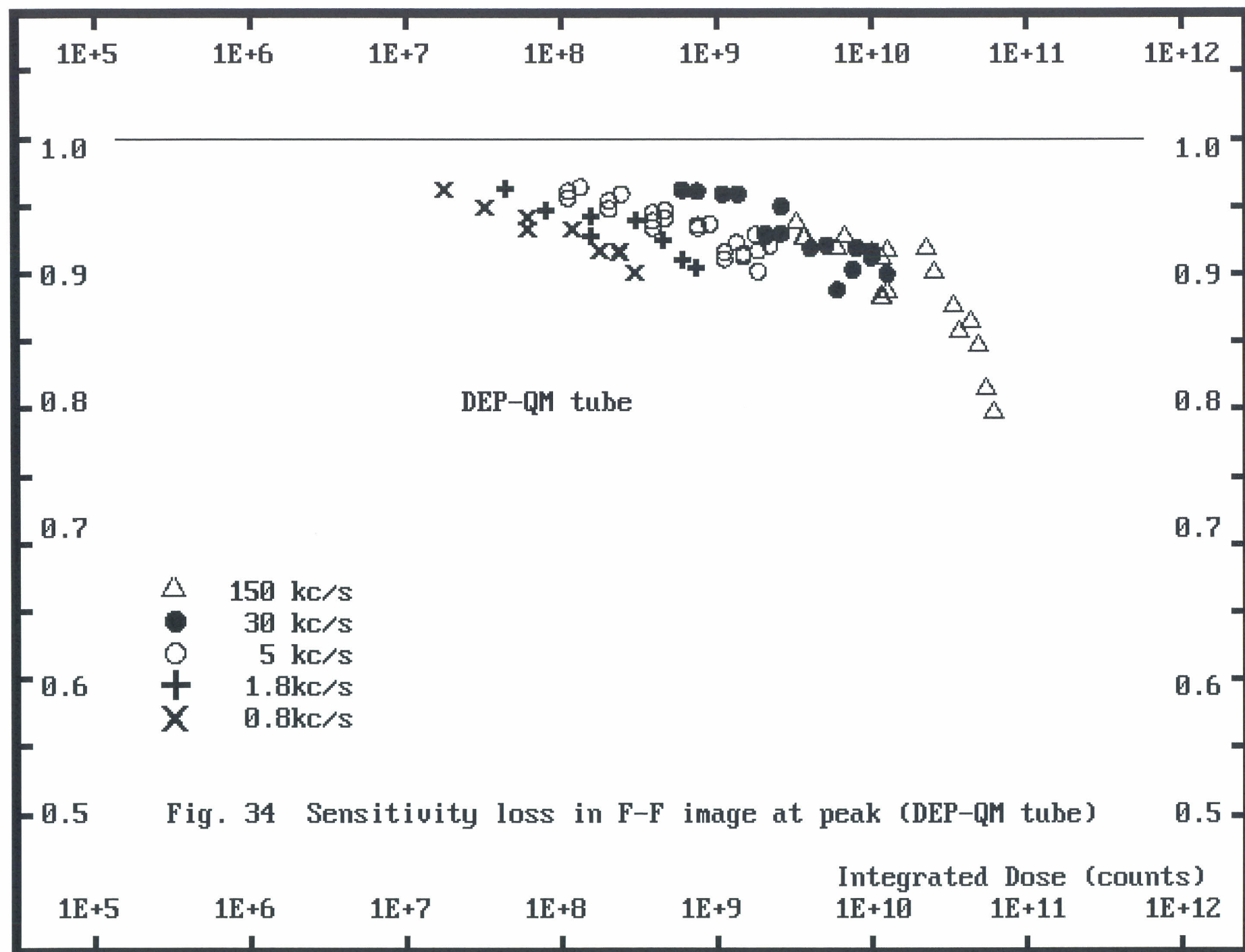
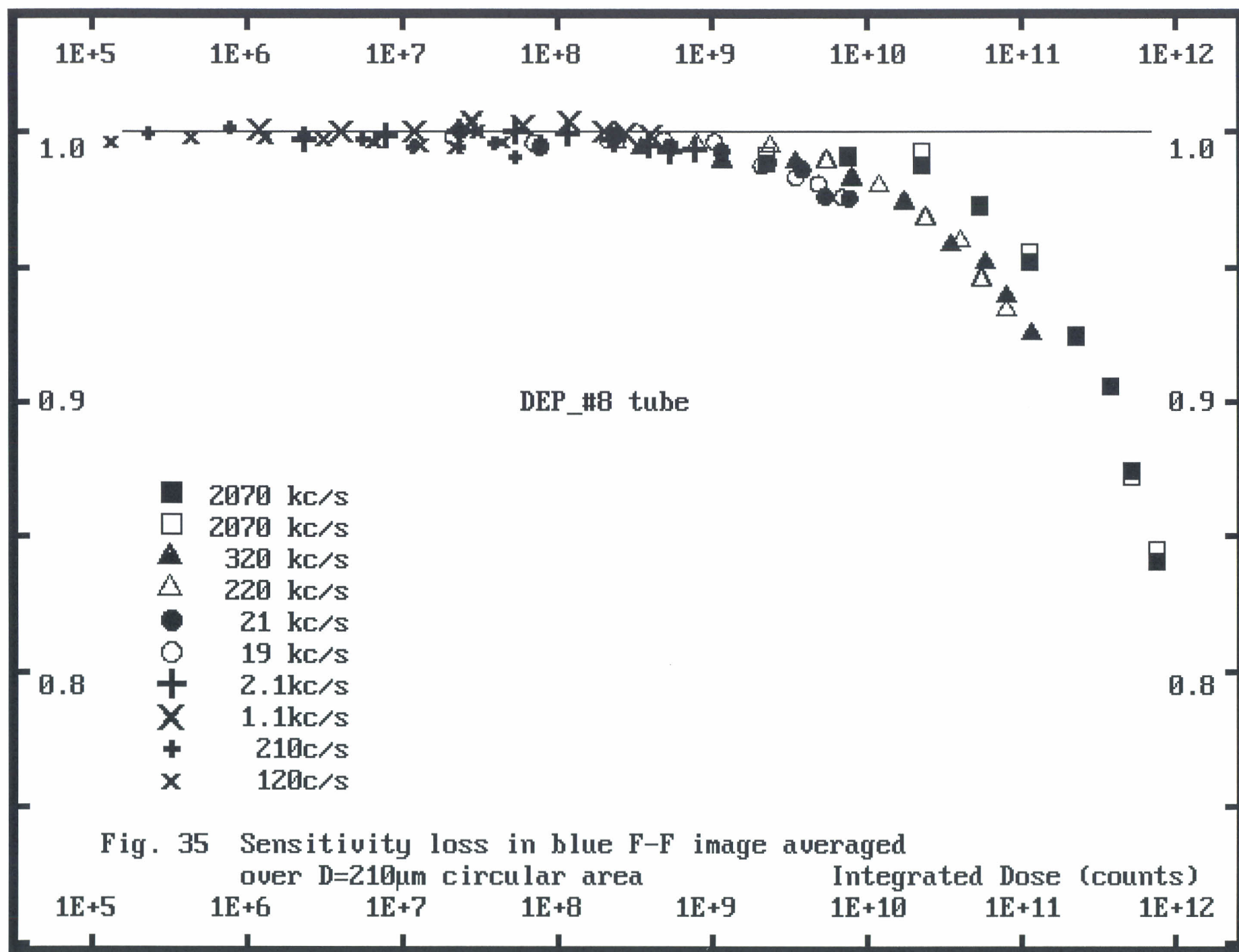
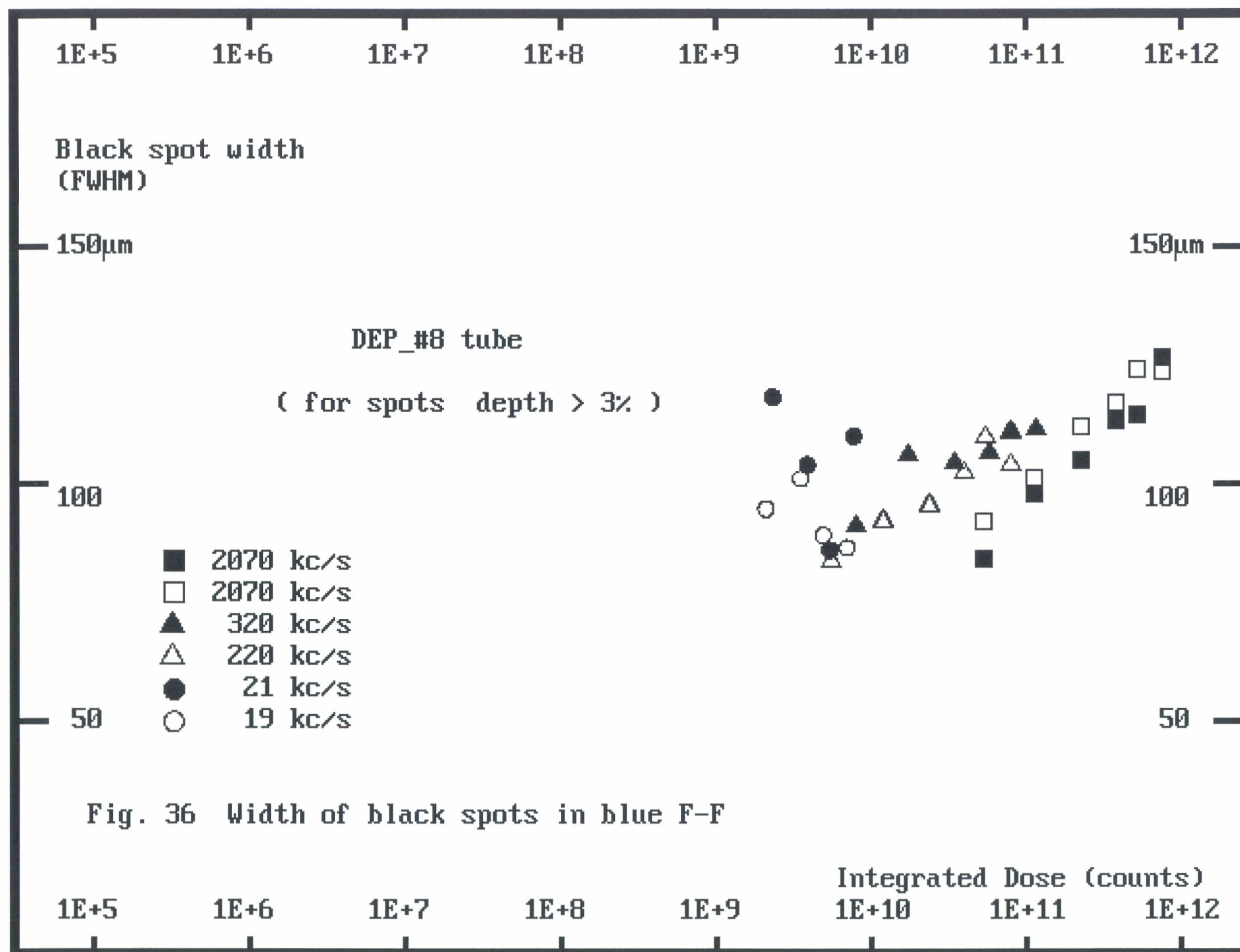


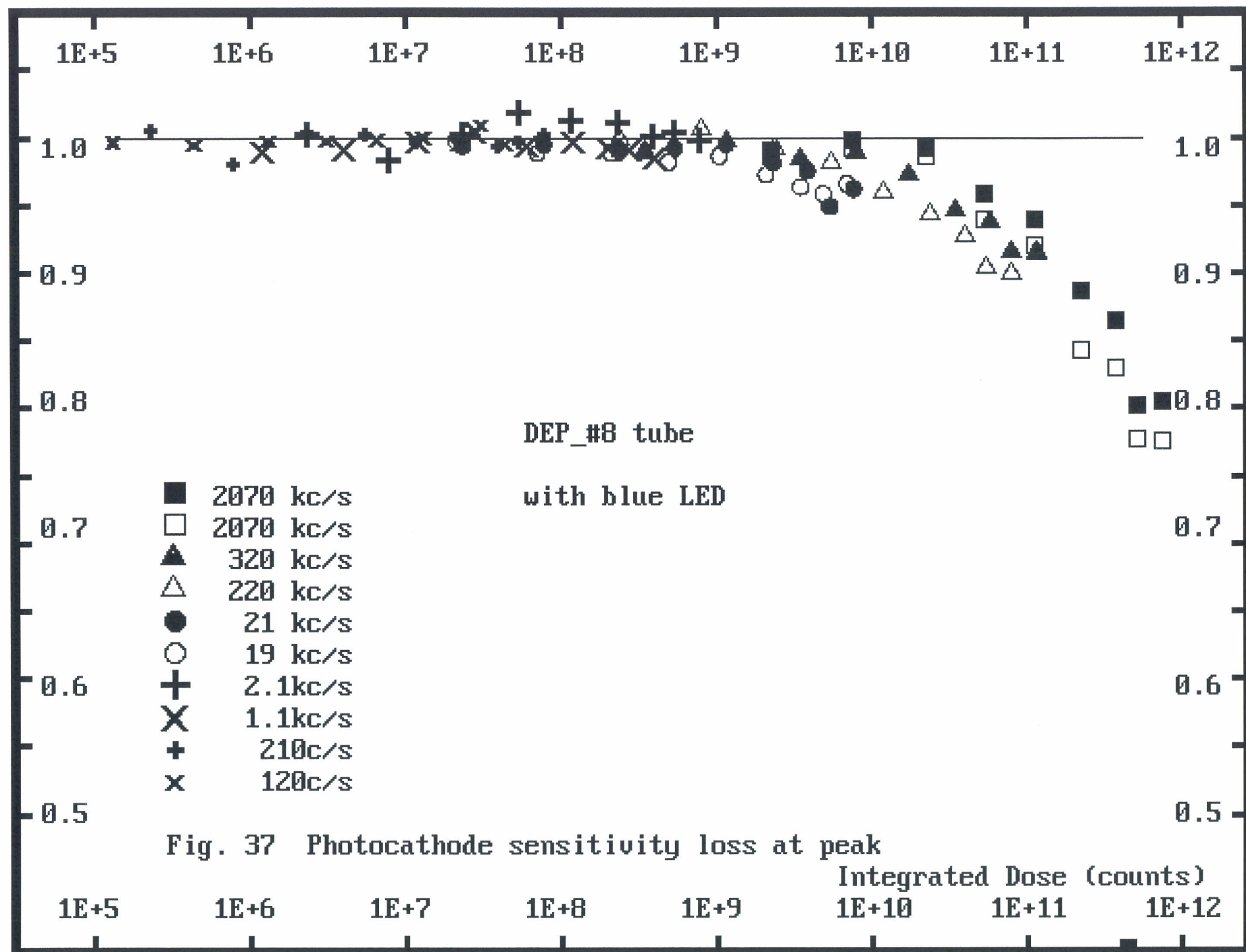
Fig. 32 Growth of sensitivity loss in F-F image with blue LED DEP_#8 tube











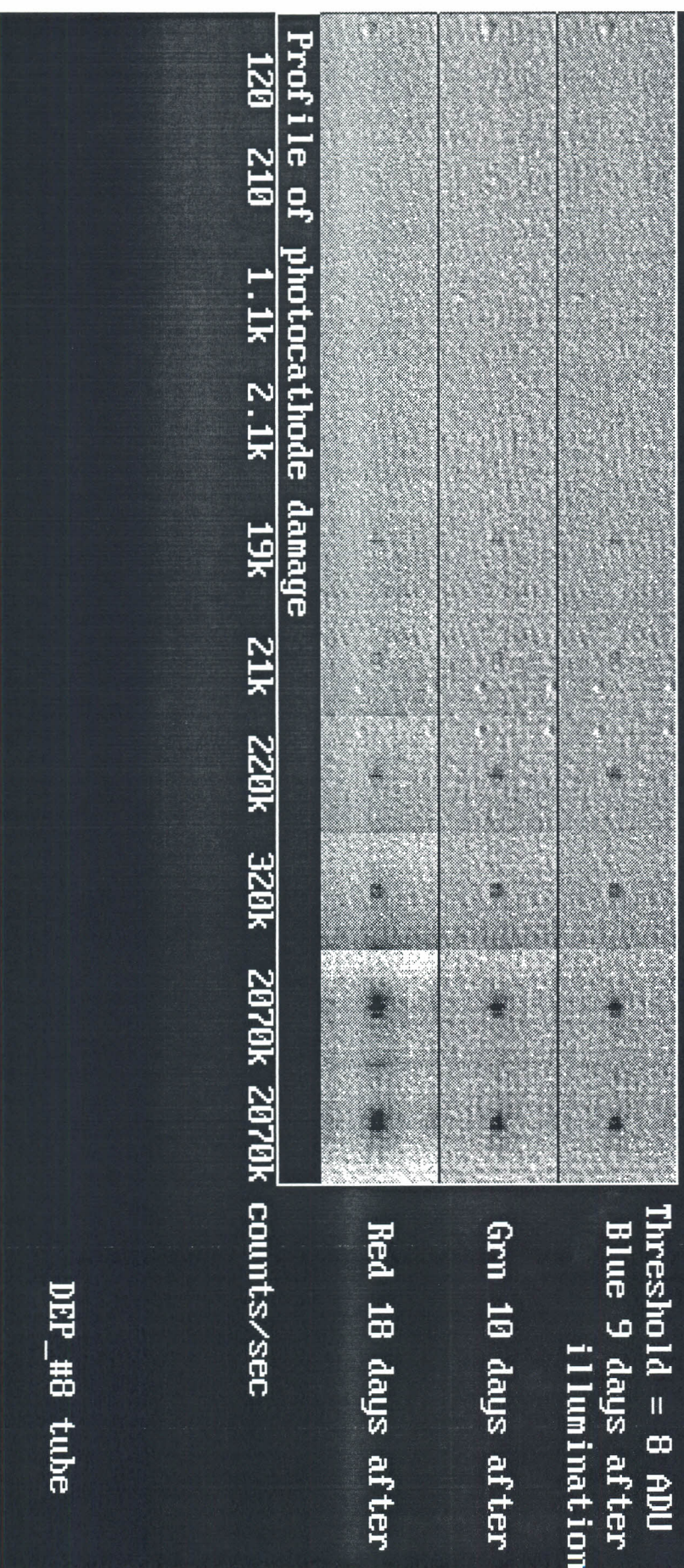
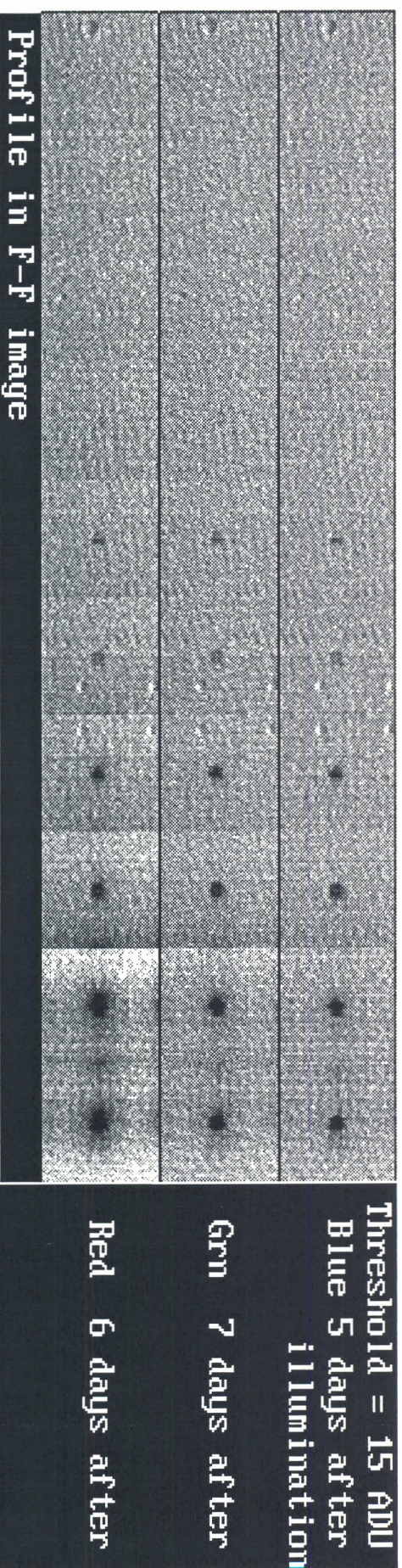


Fig. 38 Sensitivity loss in different colours Total dose = 100 hours

DEP_#8 tube

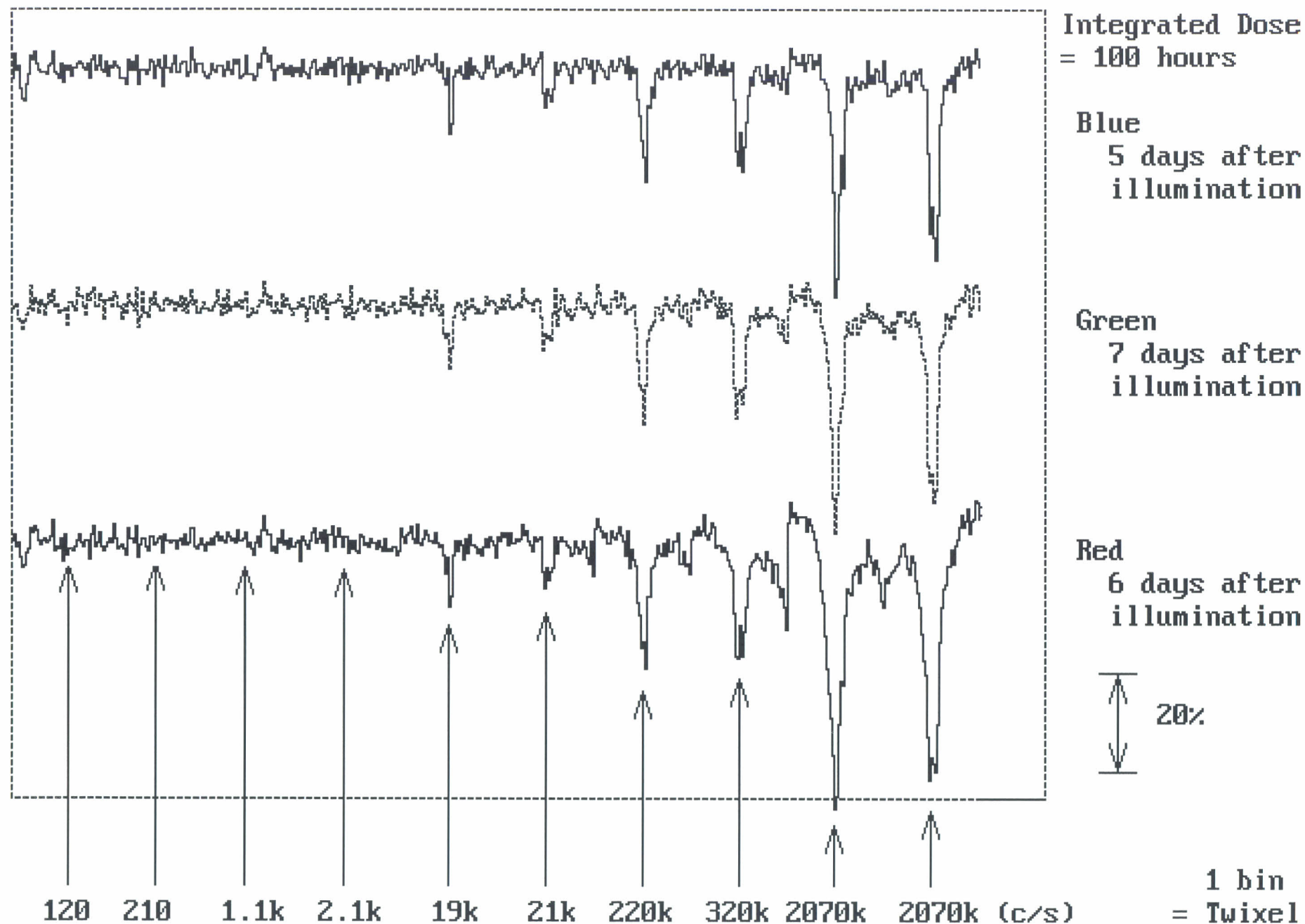
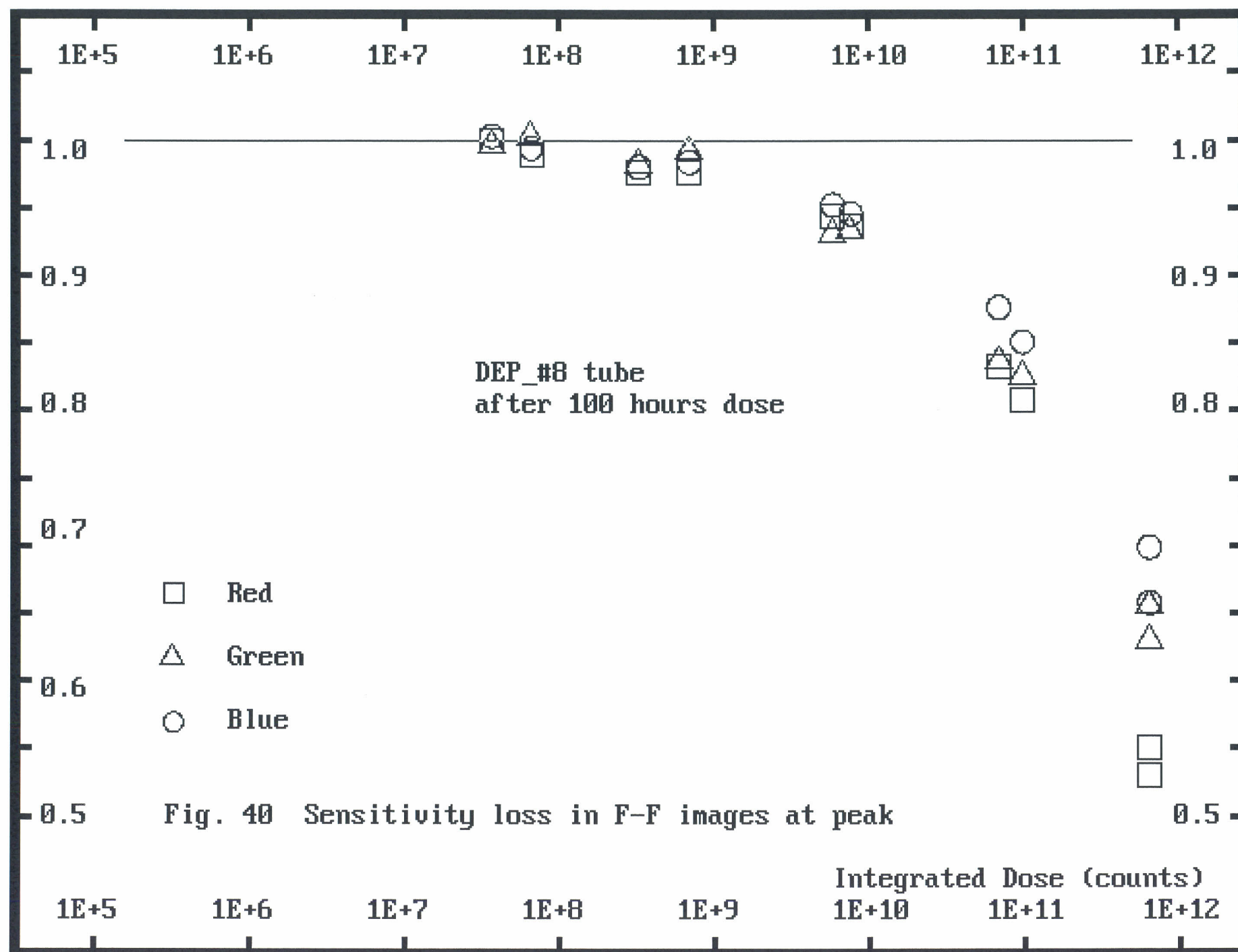
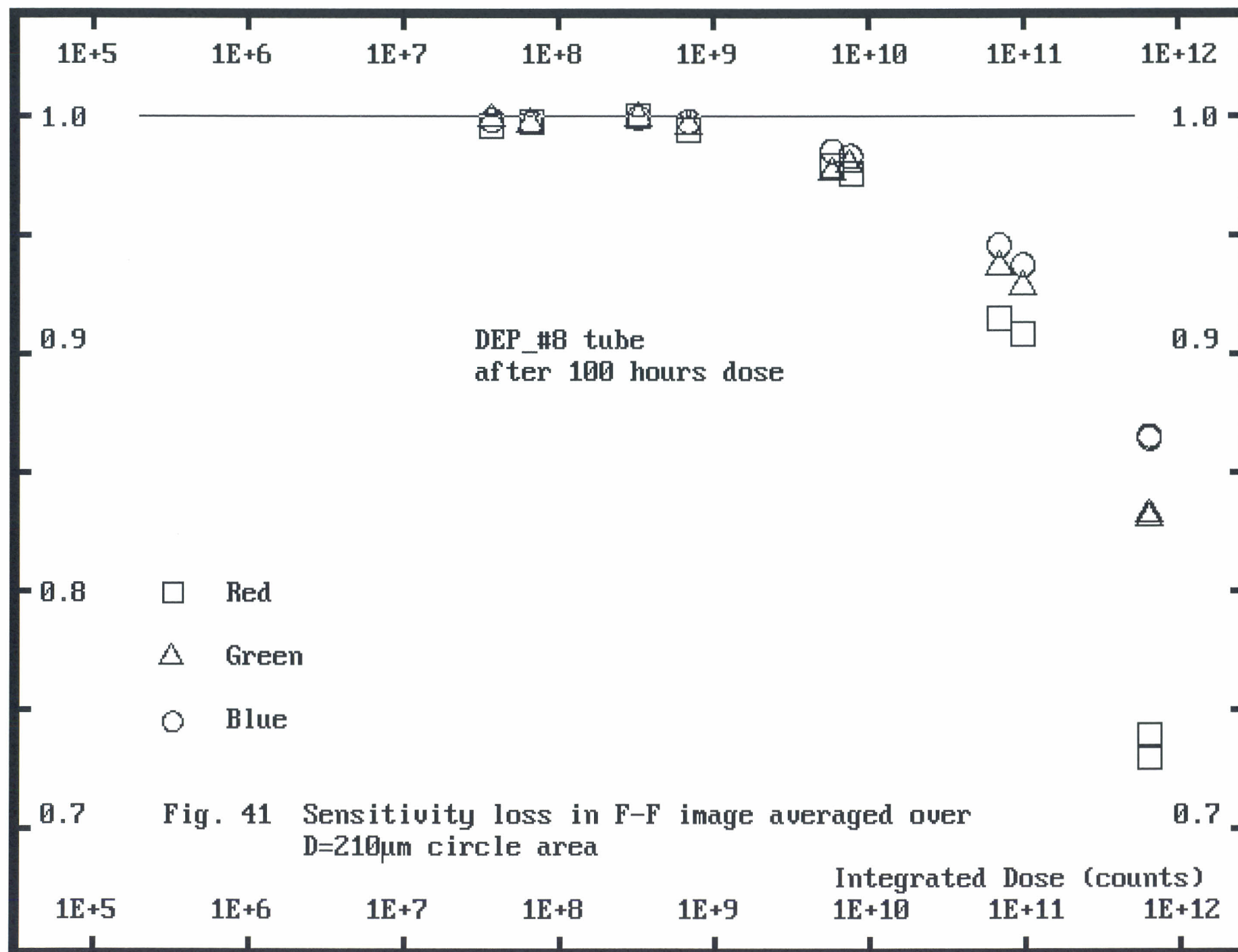
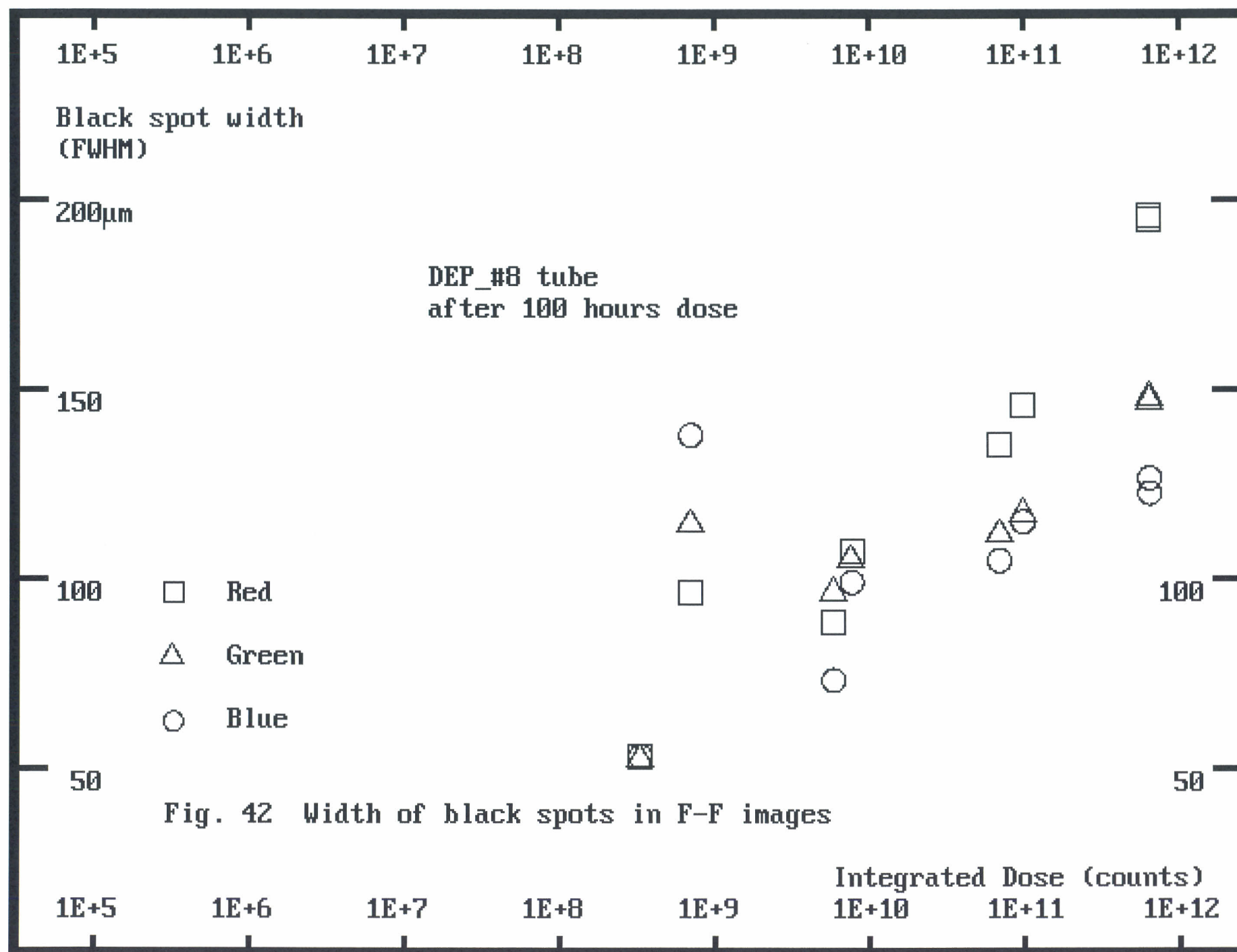


Fig. 39 Sensitivity loss in F-F image with different colours

DEP_#8 tube







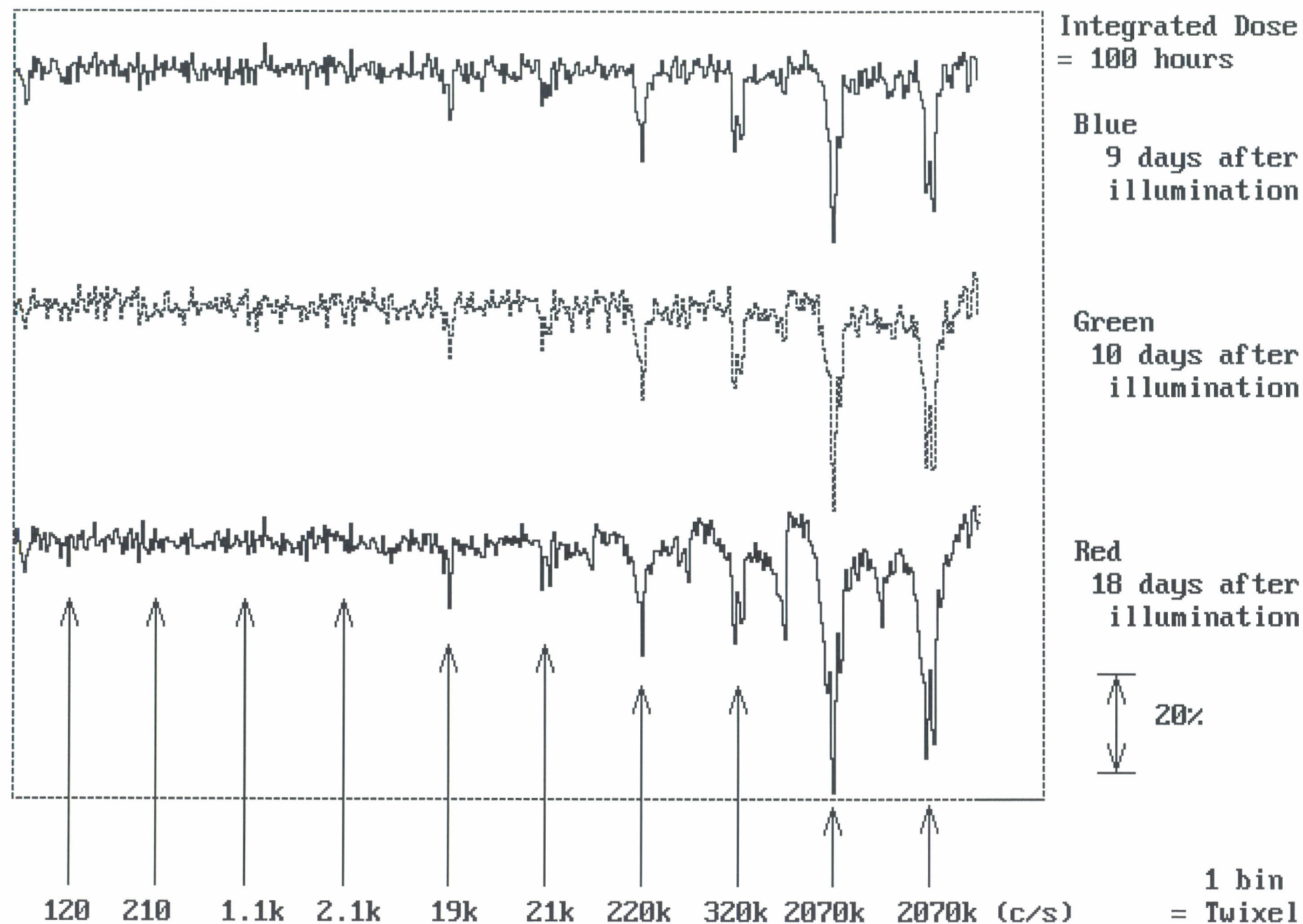
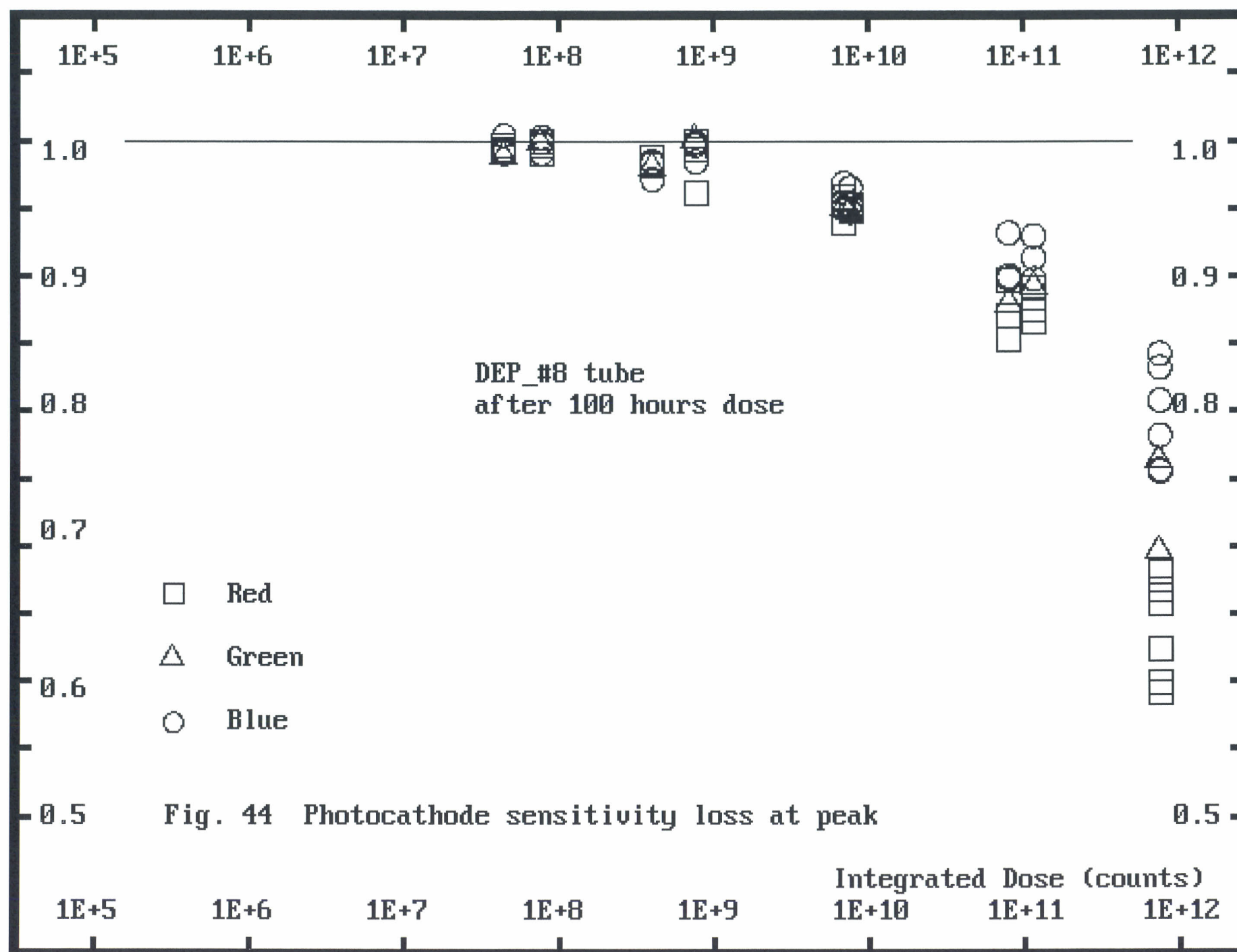
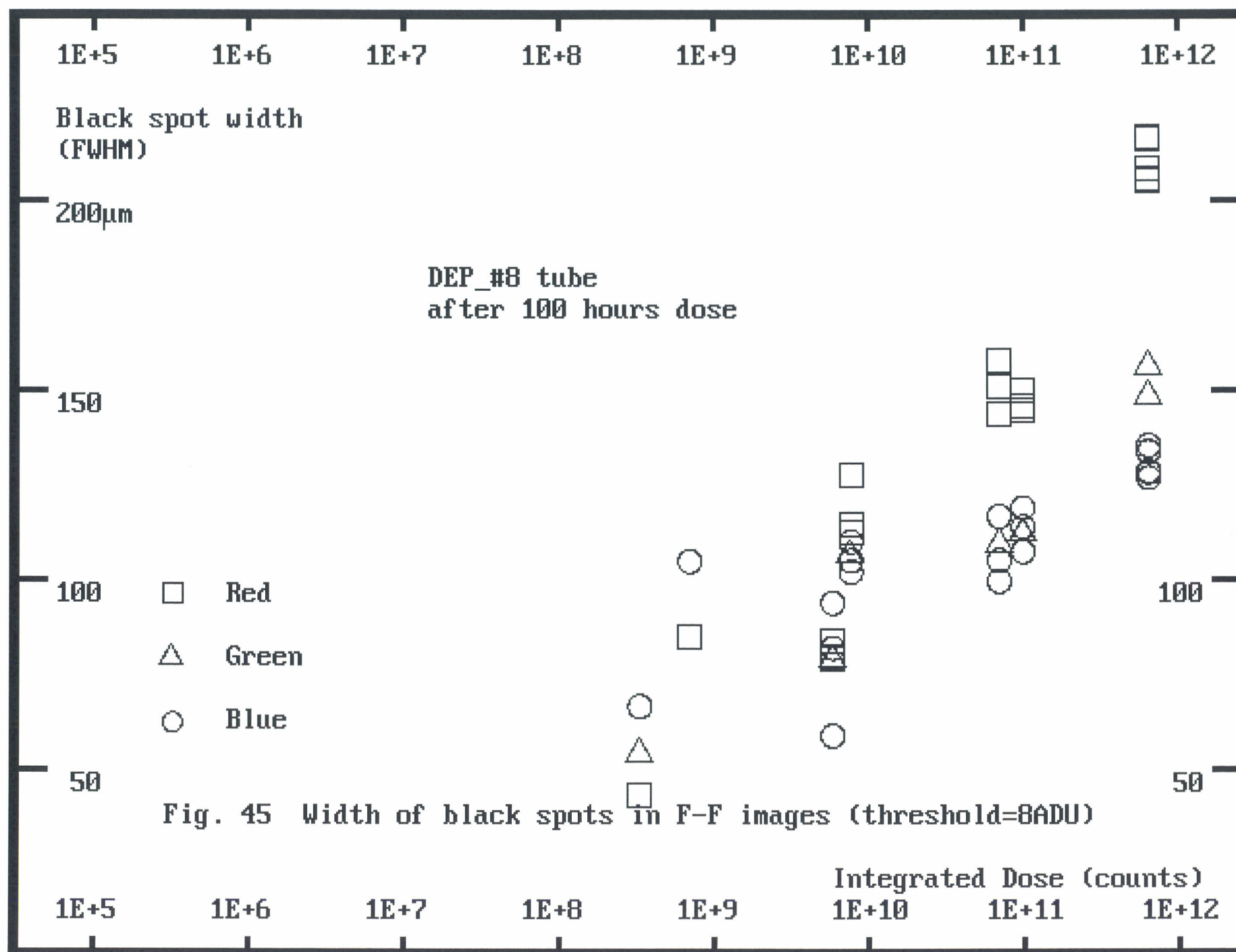


Fig. 43 Photocathode sensitivity loss in 3 colours

DEP_#8 tube





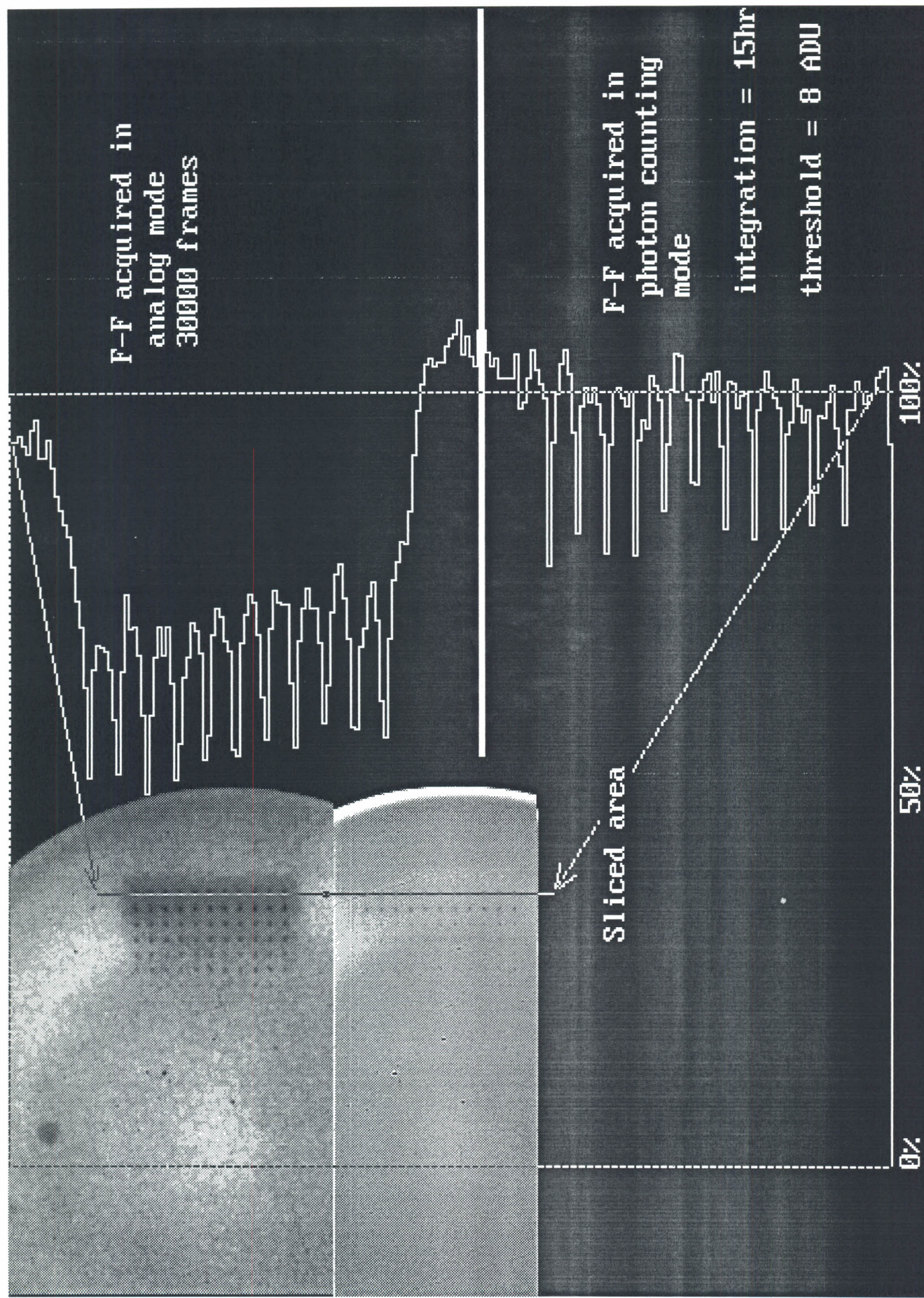
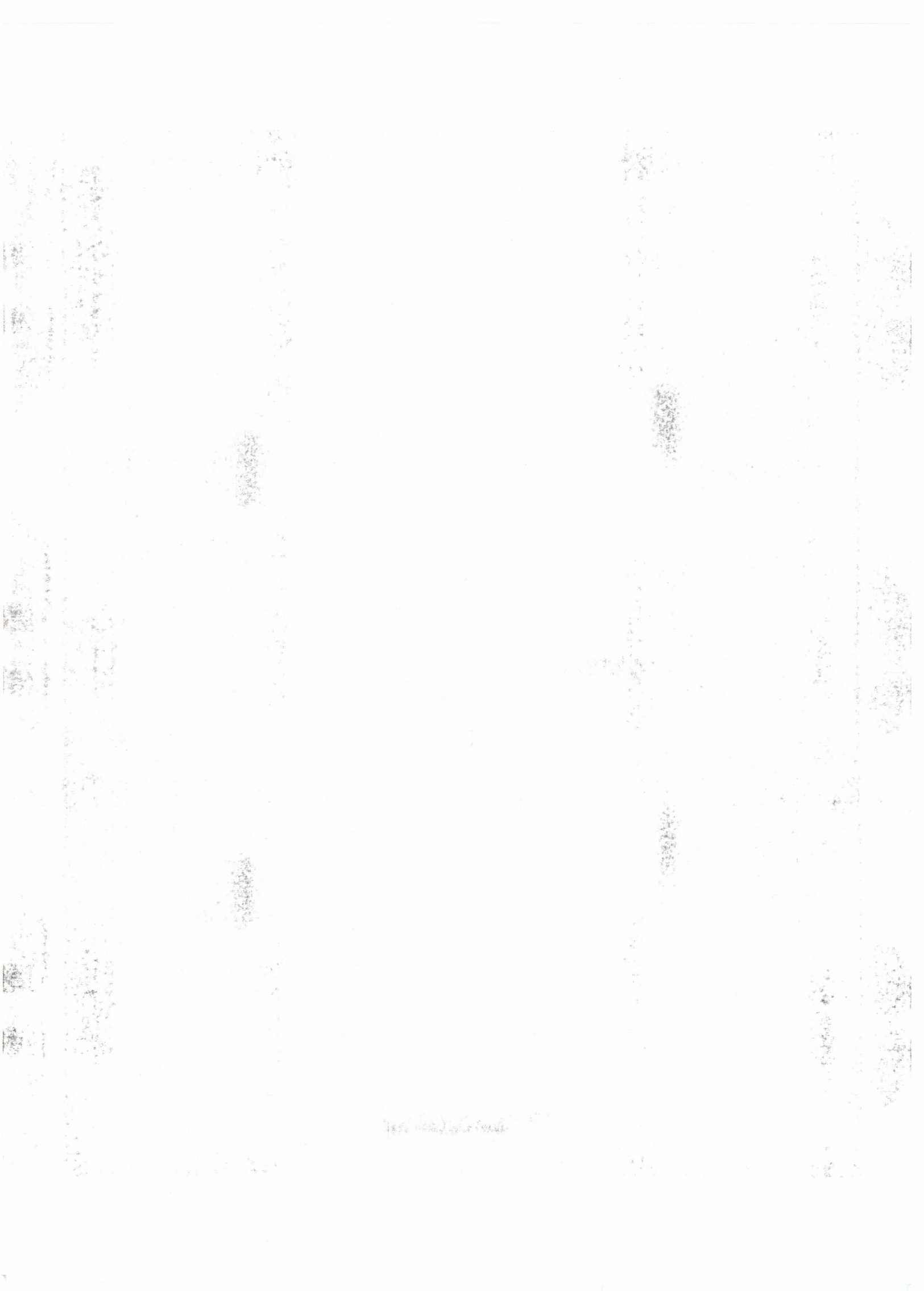


Fig. 46 Photon counting and analog F-F images, with blue Led, dose=100 hours



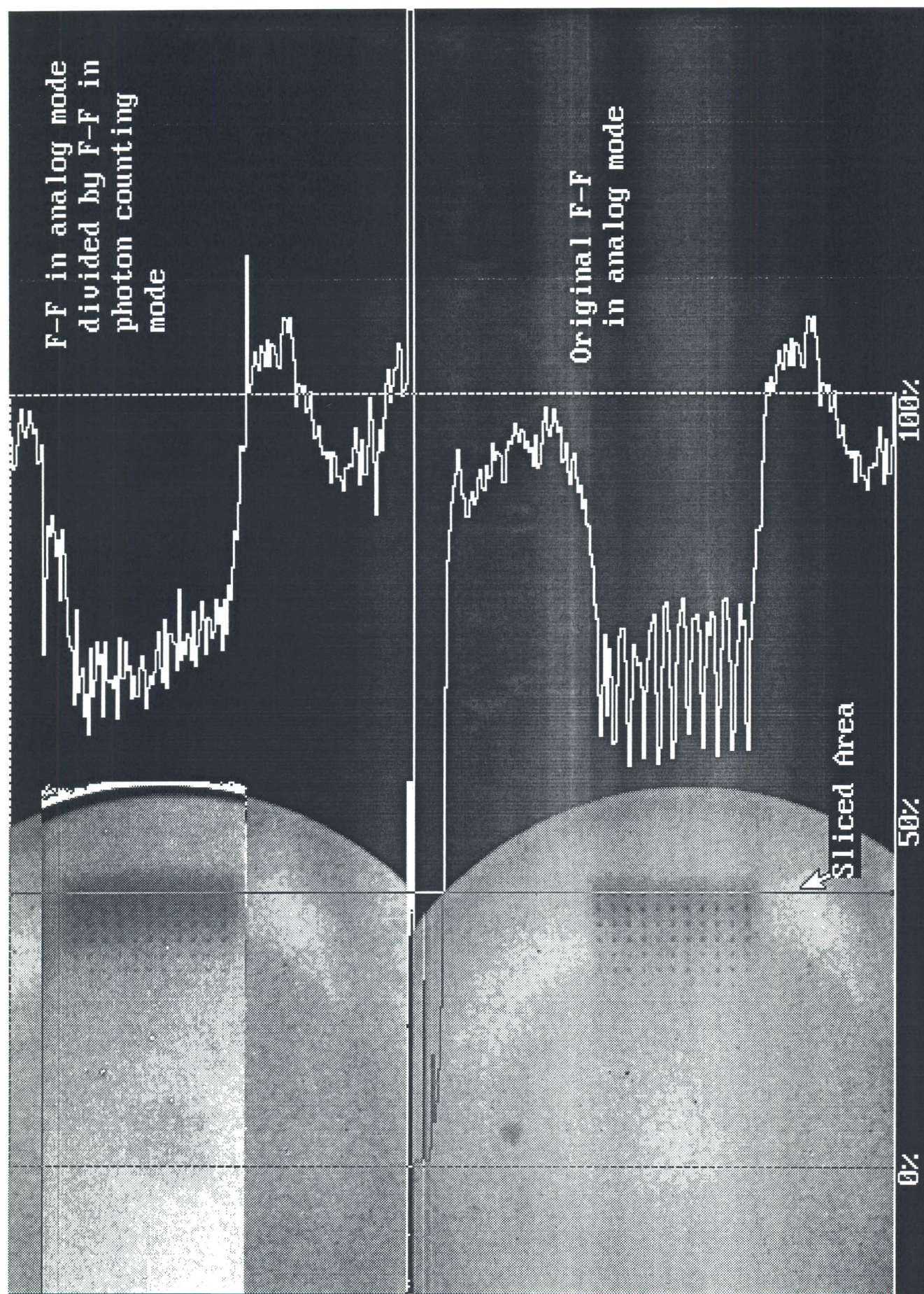
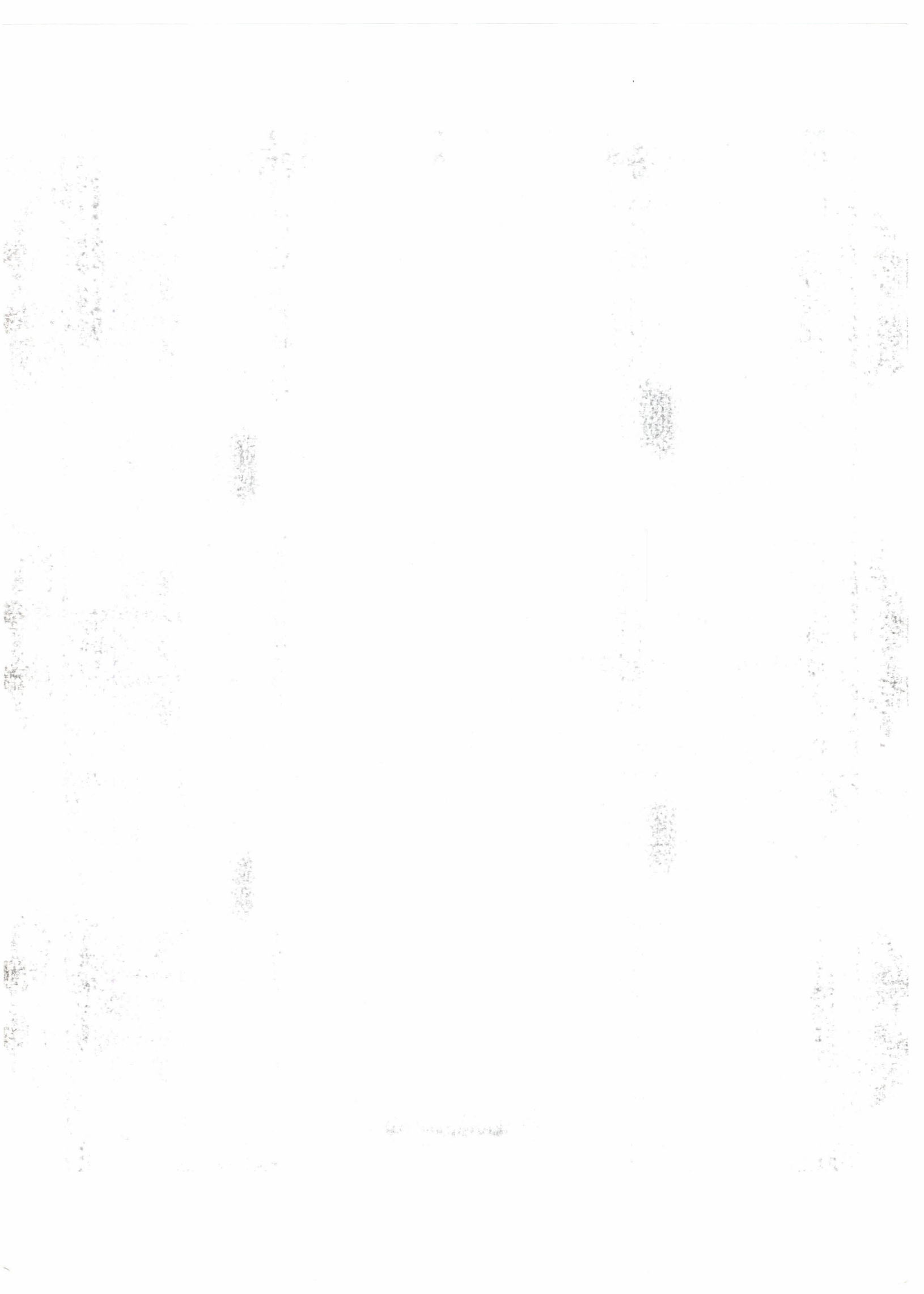


Fig. 47 Spatial extent of MCP gain depletion



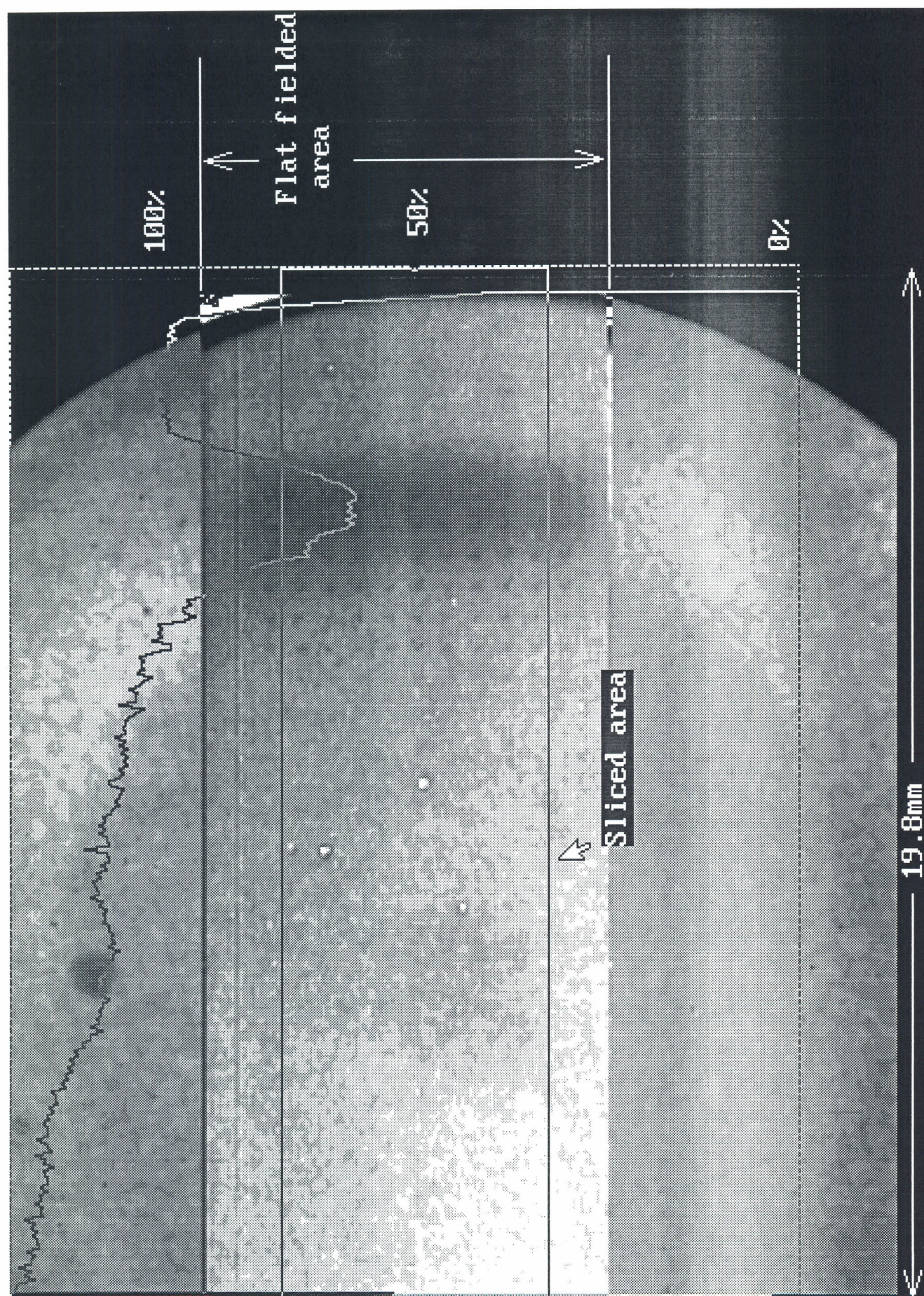


Fig. 48 Spatial distribution of MCP gain depletion Dose=100 hours

